FOSSIL FUEL RELATED WATER-ROCK INTERACTION IN THE APPALACHIAN BASIN, PENNSYLVANIA AND NEW YORK: A GEOCHEMICAL AND STRONTIUM ISOTOPE INVESTIGATION

by

Elizabeth C. Chapman

B.S. Chemistry, University of Pittsburgh, 2006

Submitted to the Graduate Faculty of

the Kenneth P. Dietrich School of

Arts and Sciences in partial fulfillment

of the requirements for the degree of

Doctor of Philosophy

University of Pittsburgh

2011

UNIVERSITY OF PITTSBURGH

FACULTY OF THE DIETRICH SCHOOL OF

ARTS AND SCIENCES

This dissertation was presented

by

Elizabeth C. Chapman

It was defended on

November 21, 2011

and approved by

Thomas Anderson, Professor, University of Pittsburgh

Harry Edenborn, Research Microbiologist, National Energy Technology Laboratories

Emily Elliott, Assistant Professor, University of Pittsburgh

Robert Hedin, President, Hedin Environmental

Brian Stewart, Associate Professor, University of Pittsburgh

Dissertation Advisor: Rosemary Capo, Associate Professor, University of Pittsburgh

FOSSIL FUEL RELATED WATER-ROCK INTERACTION IN THE APPALACHIAN BASIN, PENNSYLVANIA AND NEW YORK: A GEOCHEMICAL AND STRONTIUM ISOTOPE INVESTIGATION

Elizabeth C. Chapman, PhD

University of Pittsburgh, 2011

Fossil fuel resources (coal/oil/natural gas) have been extracted from the Appalachian Basin for over a century. Related fluids, including outflows from inactive coal mines and produced water from oil and gas wells, pose environmental concern. Three studies are presented which integrate strontium (Sr) isotopes with geologic and geochemical analyses to investigate the movement of fossil fuel-related fluids through the environment and their interactions with natural waters and geologic materials.

In the first study, abandoned oil and gas wells tapping Upper Devonian units in northwestern Pennsylvania serve as conduits for the movement of waters with high amounts of total dissolved solids (TDS). This work demonstrates that the waters originate as acid mine drainage (AMD), which infiltrates shallow, siderite-cemented sandstone aquifers. Dissolution of the siderite cement produces waters rich in dissolved iron, which flow to the surface via wells with compromised casings.

The second study focuses upon high-TDS water produced during natural gas extraction from the Middle Devonian Marcellus Shale. Strontium isotopic ratios of produced waters collected from across Pennsylvania define a relatively narrow set of values ($^{87}Sr/^{86}Sr$ = 0.71008-0.71212) that falls above that of Devonian seawater, and is distinct from most western Pennsylvania AMD and Upper Devonian Venango Formation oil and gas brines. The uniformity of the isotope ratios suggests a basin-wide source of dissolved solids. Mixing models indicate that Sr isotopes can potentially detect even small amounts (<0.01%) of Marcellus produced water interacting with natural waters.

In the third study, a sequential extraction procedure was carried out on drill cuttings from a well in south-central New York that penetrates the Marcellus Shale and adjacent units. Sr isotopic values of water and ammonium acetate leachates, representing soluble salt and clay-exchangeable fractions, fall within or just below the range measured for Marcellus produced waters, indicating that the waters’ dissolved solids originate from within the shale. Acetic acid leaches targeting carbonate minerals yield $^{87}Sr/^{86}Sr$ ratios below those of the water and ammonium acetate leaches, but higher than those expected for Devonian seawater. Rb-Sr isotope systematics suggest mixing between a seawater-derived source and more radiogenic material, and multiple generations of carbonate mineral precipitation.

TABLE OF CONTENTS

LIST OF TABLES

LIST OF FIGURES

PREFACE

I would like to acknowledge the following people for their assistance in this work: Carl Kirby of Bucknell University, for samples, data, and XRD analyses; Radisav Vidic of University of Pittsburgh's Department of Civil and Environmental Engineering, for samples and data; Rick Hammack, Hank Edenborn, and Karl Schroeder of the Department of Energy's National Energy Technology Laboratory, for providing samples of produced waters and geochemical analyses; Joe Graney and Jason Johnson of University of Binghamton, for providing core cuttings and performing XRD analysis; and Bob Hedin and Ted Weaver of Hedin Environmental, Inc., for collecting water and rock samples, sharing their knowledge of Clarion County geology, and being excellent field guides.

I would also like to thank my committee members Tom Anderson, Emily Elliott, Hank Edenborn, and Bob Hedin for their support and suggestions. Additional thanks go to Brian Stewart, in particular for performing Sr analysis of my samples on the TIMS, and in general for being a second advisor to me and supporting me and my work in countless ways. I want to express gratitude to Rosemary Capo for agreeing to be my graduate advisor. I have greatly enjoyed working with you, and appreciate all of your hard work and encouragement.

This work was supported by grants from the U.S. Department of Energy, the Green Building Alliance, and the Colcom Foundation, as well as University of Pittsburgh's Leighton Memorial Scholarship and Experiential Learning Summer Research Fellowship.

DEDICATION

This work is dedicated to my husband Charles, for his unwavering support and commitment to my goals and dreams. Ours is a story of a social worker's love for a scientist.

1.0 INTRODUCTION

The Appalachian Basin is a region which has been and continues to be a productive source of fossil fuels, including coal, oil, and natural gas. In fact, the first commercial oil well in the United States was drilled in northwestern Pennsylvania in 1859 (Giddens, 1947). Thousands of oil and natural gas wells have been drilled since that time via traditional, moderate-depth techniques that target oil and gas trapped in sandstone and limestone reservoir rocks. In the last few years, unconventional methods that involve horizontal drilling and hydrofracturing have begun to tap into deep black shale reservoirs. Coal has been mined for more than two centuries from both shallow surface and underground mines. The operation of all of these fossil fuel extraction activities within a relatively small area, combined with the complex geology of the region, creates contaminated fluids that are of significant environmental concern. In addition, exploration and remediation activities are complicated by the existence of numerous mines and wells, many of which remain undocumented. Novel and sensitive tools need to be developed and applied in order to understand water-rock interactions within this heavily mined and drilled region; to identify and remediate possible contaminant sources; to quantify the contributions of fossil fuel-related waters to ground and surface water; and to track their migration through the environment. The application of strontium isotopes is a tool that shows promise as a tracer of environmental processes in the Appalachian Basin.

1.1 GEOLOGIC SETTING OF THE APPALACHIAN BASIN

1.1.1 Basin extent and structure

The Appalachian Basin is a foreland basin comprising Paleozoic (Early Cambrian through Early Permian age) sedimentary rocks that stretch from New York to northeastern Alabama (Fig. 1). For the purposes of this dissertation, the basin is defined to include both the Appalachian Plateau and Pennsylvania Valley and Ridge physiographic provinces. The basin trends northeast-southwest and covers an area of about 480,000 km^2 (Ryder, 1995). The northwestern end of the basin dips shallowly to the southeast and extends offshore into Lakes Erie and Ontario. The eastern flank is characterized by thrust-faulted and folded rocks deformed during the late Paleozoic Alleghenian orogeny (Ryder, 1995). Most fossil fuel resources are found in the northern and central portions of the basin (U.S. EPA, 2004).

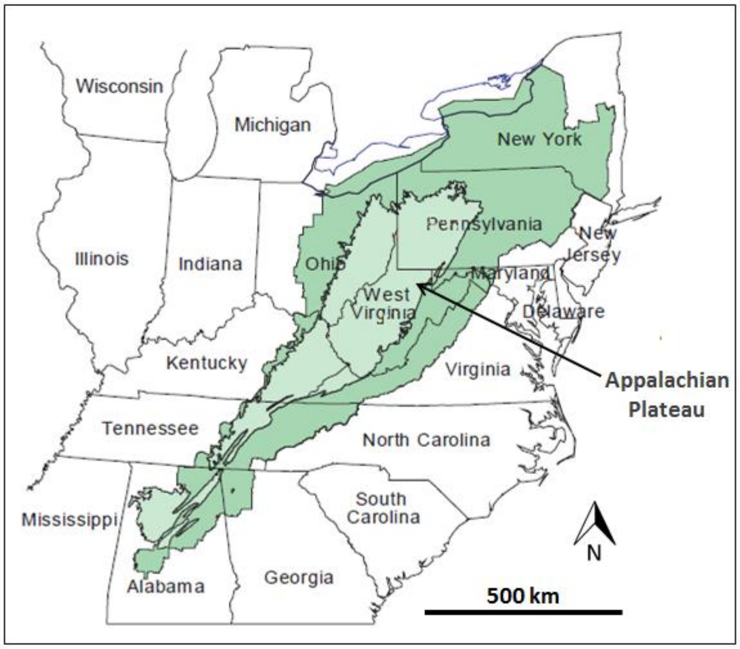

Figure 1. Appalachian Basin Province of the northeastern U.S. (shaded area). Modified from Milici and Swezey, 2006.

1.1.2 Paleozoic stratigraphy

The Appalachian Basin contains alternating siliclastic and carbonate strata from Early Cambrian through Early Permian age, with one major unit of evaporitic strata in the Upper Silurian (Salina Formation; Swezey, 2002). In this dissertation, the focus is on Middle and Upper Devonian oil and gas-producing units, and on coal units of Pennsylvanian age (Fig. 2).

In the Middle Devonian section, Onondaga Limestone is overlain by Marcellus Shale, which forms the base of the Hamilton Group. Above the Hamilton Group is the Tully Limestone, whose upper contact in Pennsylvania is an unconformity. Most Upper Devonian units, including the Elk, Bradford, and Venango sandstones and siltstones, are included within the Catskill Formation. Pennsylvanian units include, from oldest to youngest, the Pottsville and Allegheny Formations and the Conemaugh and Monongahela Groups (Swezey, 2002).

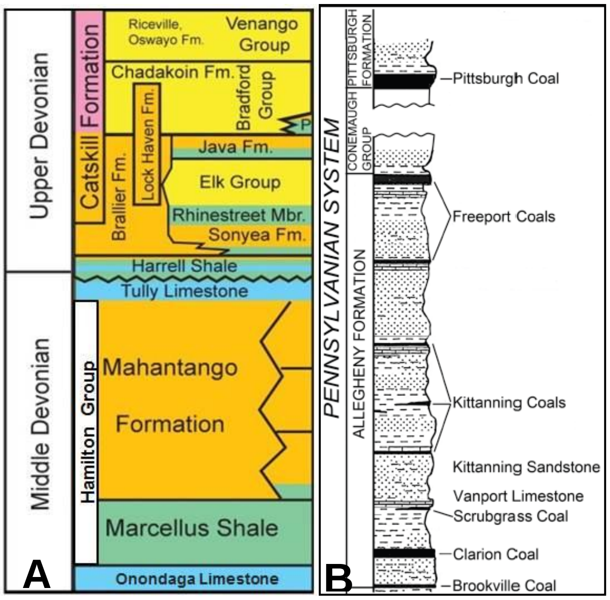

Figure 2. Generalized stratigraphy of western Pennsylvania. A: Middle and Upper Devonian, modified from Milici and Swezey, 2006. B: Pennsylvanian coal-bearing strata.

1.1.3 Fossil fuel resources

1.1.3.1 Conventional oil and gas

Conventional oil and gas drilling in the Appalachian Basin began in 1859 when oil was discovered at the Drake Well in Venango County, Pennsylvania. Since then, a number of producing sandstone and limestone reservoirs have been identified in Upper Cambrian through Pennsylvanian strata. Some of the largest oil fields have been developed in the Bradford (Upper Devonian), Clinton (Lower Silurian), and Big Injun (Lower Mississippian) sands; large gas fields include the Big Sandy (Mississippian and Pennsylvanian), Oriskany (Lower Silurian), Medina (Lower Silurian), and Venango (Upper Devonian) sands (Ryder, 1995).

In the 150 years since the first oil well was drilled in the Appalachian Basin, approximately 325,000 more have been drilled in Pennsylvania alone (PA DEP, 2000). Over 70% of these wells are thought to be abandoned, and less than 20% of these abandoned wells are known to be plugged (PA DEP, 2000). Abandoned wells can serve as conduits for contaminated water and methane leaks (Baldassare and Laughrey, 1997; CA DOC, 1986; Chapman et al., in prep; Chilingar and Endres, 2005; Hedin et al., 2005; PA DEP, 2007).

1.1.3.2 Coal

The Appalachian Basin is recognized as one of the most important coal-producing regions in the world (Chesnut, 1996). For over 200 years, coal has been mined from six major bituminous coal zones in western Pennsylvania; these are (from oldest to youngest): Brookville-Clarion, Kittanning, Freeport, Pittsburgh, Sewickley, and Waynesburg (Fig. 2b.). These units are all of Pennsylvanian age, and are contained in the Allegheny Formation and Monongahela Group (U.S. EPA, 2004). The depositional environments of the coal overburden trends from marine in the lower Allegheny Formation to freshwater in the Monangahela Group (Brady et al., 1998). Coal in this region is mined by both surface and deep-mine techniques (Hawkins, 1998; Perry, 2001).

1.1.3.3 Unconventional black shale gas

Of the four shale gas basins in the Appalachian Basin (Utica, Marcellus, Chattanooga, and Conasauga; GWPC and ALL Cons., 2009), the Middle Devonian-aged Marcellus Shale is the most geographically expansive, spanning large portions of West Virginia, Pennsylvania, and New York. The Marcellus is a black, organic-rich shale that was formed under anoxic conditions following the Acadian orogeny (416-359.2 Ma; Kargbo et al., 2010; Lash and Engelder, 2009). This unit reaches a thickness of up to 152 m and has an areal extent of over 13 million hectares (Engelder et al., 2009).

Because the Marcellus is a deep (>2700 m; Lash and Engelder, 2011) shale with low permeability, horizontal drilling and hydrofracturing techniques must be employed to economically recover the gas. In horizontal drilling, a vertical drill hole is turned 90° on reaching the target horizon, and then continues horizontally through that unit for as far as 1,800 m (Harper, 2008). Horizontal drilling allows for a single well to come into contact with more of the reservoir rock, thereby decreasing drilling expenses and surface disturbance from well pads (GWPC and ALL Cons., 2009).

Hydrofracturing is a method used to create additional permeability which allows gas to flow more freely from a low-permeability producing formation (Veatch Jr. et al., 1989). After the well casing is perforated, hydrofracturing fluid is pumped down-well at a pressure that exceeds the tensile strength of the rock (Kargbo et al., 2010). Hydrofracturing fluid is primarily water, with added constituents that act as proppants, scale inhibitors, biocides, and lubricant (Arthur et al., 2008). In order to hydrofracture a well, two to four million gallons of hydrofracturing fluid are used, and a portion of this fluid flows back out of the well as produced water over the lifetime of the well (estimates range from 30 to 70%; GWPC and ALL Cons., 2009).

1.2 ENVIRONMENTAL ISSUES

1.2.1 Surface water

Fossil fuel-extraction activities in the Appalachian Basin have had a significant impact on the quality of surface water in the region. Both net-alkaline and acidic mine drainage (AMD) from underground and surface coal mines affect more than 8,000 km of streams in Pennsylvania alone (Cravotta III et al., 1999). Additionally, there have been two major instances of stream contamination in western Pennsylvania since 2008, where high levels of total dissolved solids (TDS) were measured. In 2008, high TDS were measured in the Monongahela River, and in 2009 a significant fish kill took place in southwestern Pennsylvania’s Dunkard Creek. Both events were tied to influxes of AMD and/or Marcellus produced water (PA DEP, 2009; PFBC, 2011; Renner, 2009b).

Surface water contamination can also result from hydrofracturing fluid and produced water releases from Marcellus Shale well pads. Three such releases took place at a single pad in Susquehanna County, Pennsylvania, in 2011 (NYSDEC, 2011). In addition, produced water can potentially be released into the environment by spills during transport or from overflow of storage ponds during heavy rains (Zoback et al., 2010).

1.2.2 Groundwater

Groundwater contamination can also take place through a variety of processes. AMD can seep into shallow aquifers through fractures and cause widespread contamination of drinking water (Chapman et al., in prep; Hedin et al., 2005). Additionally, produced water from oil and gas drilling stored in impoundment ponds may seep into underlying ground layers; this is also a potential risk for coal fly ash impoundments (Spivak-Birndorf et al., in press; Zoback et al., 2010). Surface spills, as mentioned above, can also infiltrate shallow soil and rock units. Another potential risk of groundwater contamination is fluid or gas flow through compromised casings of modern and legacy oil and gas wells (e.g., Chapman et al., in prep; Osborn et al., 2011a).

1.3 PREVIOUS WORK

1.3.1 Geophysics

Previous work in identifying potential sources of contamination from fossil fuel-related activities employed a variety of tools, such as remote sensing and geophysical techniques, geochemical analysis, and stable isotope tracers. In the Appalachian Basin, remote sensing tools have been used to locate abandoned wells and identify possible zones of natural gas accumulation and migration (Harbert and Kaminski, 2007); detect potential environmental hazards at coal mine impoundments (Hammack et al., 2010); and locate mine pools and AMD discharges (Love et al., 2005).

1.3.2 Geochemistry

Geochemical analysis has been applied in the Appalachian Basin to study a variety of coal, oil, and gas-related issues; however, its limitations have been noted by researchers. For example, Hedin et al. (2005) proposed that shallow AMD was flowing from abandoned oil and natural gas wells in Clarion County, PA, but geochemistry alone was not sufficient to confirm that siderite dissolution was the source of iron in the gas well discharges, nor where the siderite dissolution was taking place. In other studies, researchers have suggested that Br concentrations or Br/Cl ratios may be effective tracers of Marcellus Shale produced waters (Kight and Siegel, 2011; Wilson and VanBriesen, 2011). However, Figure 3 illustrates that Br/Cl ratios do not distinguish between produced waters from different formations. And finally, Blauch et al. (2009) used mineralogical analysis of the Marcellus Shale together with the chemical composition of produced water in an attempt to determine the source of salts in the produced water. While they were able to draw some conclusions as to the nature of the salts, they also highlighted the need for further studies such as isotopic analysis to provide more information.

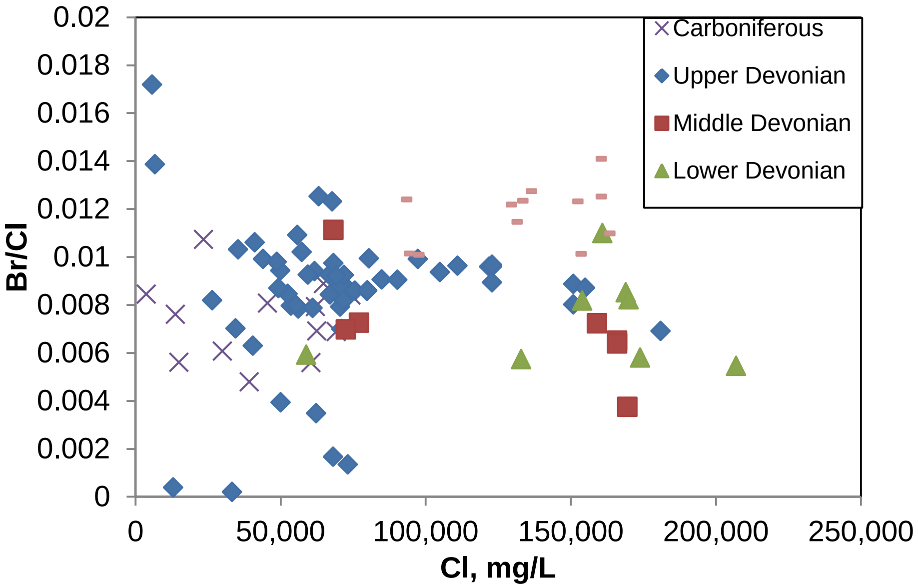

Figure 3. Br/Cl vs. Cl concentration for Appalachian Basin brines of different ages. Data from Dresel and Rose (2010), Poth (1962), and this work.

1.3.3 Stable isotopes

Stable isotopes of carbon, hydrogen, sulfate, and oxygen have been used to track fossil fuel-related fluids in the Appalachian Basin. Osborn and McIntosh (2010) analyzed C isotopes in gas and formation waters in reservoir sandstones and black shales across the northern part of the basin, concluding that most of the methane in this region is thermogenic in origin. Osborn et al. (2011a) used carbon isotopes of methane to detect contamination of drinking water and suggest a possible link between shale gas extraction by hydraulic fracturing and elevated methane concentrations in groundwater, although this has been controversial (Osborn et al., 2011b; Saba and Orzechowski, 2011; Schon, 2011). Other researchers are using a multi-stable isotope (O, H, S, and C) approach to distinguish between Marcellus produced waters and other sources of high TDS (Sharma et al., 2011). In another region of the country, Wyoming's Powder River Basin, stable isotopes have been applied to study fluids related to coalbed methane. Sharma and Frost

(2008) utilized C isotopes to track the interaction of produced water with surface water, specifically in cases where the produced water is reused in agriculture, as well as to distinguish produced water from different coal zones.

1.4 STRONTIUM ISOTOPE SYSTEM

One of the reasons that elemental concentrations are not always useful as tracers is that they can be affected by numerous environmental processes, including evaporation, temperature change, oxidation, ion-exchange or sorption processes, dilution, and mixing of waters. These processes may also significantly fractionate light, stable isotope ratios such as C, H, O, N, and S. Because of these processes, identification and quantification of water sources may be challenging. Additionally, it is difficult to understand interactions with sediments along flowpaths using chemical concentrations alone.

Conversely, these environmental processes have a negligible effect on the isotopic composition of the heavier isotopes of Sr. Naturally occurring Sr has four stable isotopes: ^{88}Sr, ^{87}Sr, ^{86}Sr, and ^{84}Sr. Additional ^{87}Sr is formed by the slow, natural decay of ^{87}Rb (half-life of 48.8 Ga). During sedimentation or diagenesis, a sedimentary rock takes on a particular ^{87}Sr/^{86}Sr ratio; this ratio increases over time, especially in very old rocks with high Rb/Sr ratios. Because of this, rock units with different geologic compositions and histories will have different ^{87}Sr/^{86}Sr ratios. Rocks with higher ^{87}Sr/^{86}Sr ratios are said to be more radiogenic (because they contain more ^{87}Sr produced by decay of ^{87}Rb).

Strontium isotope signatures in ground and surface waters are primarily controlled by the balance of dissolved inputs. As water interacts with sediments and rocks, it can dissolve Sr-containing minerals and adopt their $^{87}Sr/^{86}Sr$; and because rain and snowfall in non-arid regions such as the Appalachian Basin generally have very low Sr concentrations (<50 μg/L), the Sr composition of ground and surface waters reflects the aquifer matrix and allows for tracing of aquifer processes (Graustein, 1989).

1.5 STRONTIUM ISOTOPES AS A TRACER OF WATER-ROCK INTERACTION

Strontium isotopes effectively reveal water-rock interactions and are used to identify and quantify contaminant sources (Banner et al., 1994; Bayless et al., 2004; Brinck and Frost, 2007; Christian et al., 2011; Jiang et al., 2009; Leung and Jiao, 2006). For example, Frost et al. (2002) used Sr isotopes in Wyoming's Powder River Basin to distinguish groundwater whose source is a sandstone aquifer from waters originating in coal seams. They found that groundwater from coal seams has higher and more variable $^{87}Sr/^{86}Sr$ ratios than sandstone waters. They also observed that $^{87}Sr/^{86}Sr$ ratios increased with increasing water-rock interaction along flowpaths in the subsurface. Hamel et al. (2010) applied Sr isotopes in a situation where acid mine drainage was interacting with coal combustion byproducts in a grouted mine. Using Sr isotopic ratios, the authors were able to determine which waters were interacting with the grout, as well as estimate the rate of grout dissolution.

In both of these examples, major and trace element geochemistry alone failed to clearly show the sources and interactions of the studied waters. Hamel et al. (2010) found that the geochemistry was not sufficient to differentiate between discharges from grouted and non-grouted areas. While K, As, and Cu showed the most promise in distinguishing the waters, they still had overlap between waters which had interacted with the grout and waters which had not.

They concluded that interaction with the grout did not significantly change the geochemistry of the waters. Frost et al. (2002) found that neither major ion geochemistry nor oxygen and hydrogen stable isotopes revealed the source of groundwater. They found that waters from coal and sandstone aquifers were both of meteoric origin, and therefore their O and H stable isotopic signatures are indistinguishable. Additionally, the waters from coal aquifers are primarily of sodium bicarbonate type, which is also true of the waters from deep sandstone aquifers in that region. As a result, major ion geochemistry was not useful in determining the waters' sources.

Strontium isotopes also may be used to distinguish between natural and anthropogenic sources of major elements, as well as the effects of mixing water from different sources. Frost and Toner (2004) used Sr isotope analysis of groundwaters to identify extensive interaction of waters between different Wyoming aquifers in an area where major-ion approaches had failed. Leung and Jiao (2006) were able to use Sr isotopes to identify leakage from drinking water mains when major and trace geochemistry was not sufficient to distinguish municipal drinking water from natural groundwater. By combining Sr isotopic ratios with major element geochemistry (NO_3^- concentrations; Mg/Sr and Ca/Sr molar ratios) and ^3H values, Brenot et al. (2008) were able to track fertilizer contributions to shallow groundwater in a small agriculture catchment (3 km^2) in north-central France.

1.6 RESEARCH OBJECTIVES AND APPROACH

The major objectives of this research are to identify and quantify contamination from fossil fuel-related waters, and to clarify the role that sediments and rock units play in this process. Specifically, the goals of this dissertation are to (1) identify sources of high-TDS water contamination in coal mining and oil and gas drilling areas; (2) understand the source and form of these dissolved solids; (3) characterize AMD and oil and gas produced waters; and (4) identify and quantify mixing and dissolution processes which may take place along flowpaths. These objectives were accomplished in three case studies using an integrative approach that included Sr isotope analysis, major and trace element geochemistry, mineralogy, and knowledge of local stratigraphy and hydrogeology.

1.7 ORGANIZATION OF THIS DISSERTATION

Results of the three studies that form the basis of the dissertation research are presented in Chapters 2, 3, and 4, which are structured as manuscripts for submission to peer-reviewed journals. The material presented in Chapter 2 is being revised for *Applied Geochemistry*; that in Chapter 3 has been submitted to *Environmental Science & Technology*; and Chapter 4 is in preparation for submission. Chapter 5 provides conclusions and suggests future work in this subject.

The field locations for this research span a number of counties in New York and Pennsylvania: Tioga County, NY, and Bradford, Clarion, Westmoreland, Washington, and Greene Counties, PA. At each location, Sr isotopes were applied to understand and track the interaction of fossil fuel-related waters with geologic strata. Information about stratigraphy and subsurface structure was applied at each site to interpret isotopic results. In addition to Sr isotopic data, major and trace element geochemistry was employed in a multi-proxy approach to identify subsurface processes and distinguish fossil fuel waters from natural surface and groundwater.

The first project is an investigation of iron-contaminated artesian discharges from numerous abandoned natural gas wells in northwestern Pennsylvania that pollute nearby streams and forests. Typically, the source of water flowing from abandoned wells is derived from brines produced from the oil and gas-bearing strata; the discharges in the study area, however, have geochemistry similar, but not identical, to that of coal AMD. Hedin et al (2005) used major and trace geochemistry of a number of these iron-rich discharges, along with AMD discharge chemistry in the area, to propose that the geochemical differences were due to AMD's interaction with the iron carbonate mineral siderite ($FeCO_3$) that is found in both the mine spoil and subsurface aquifers. This iron source was confirmed through the application of Sr isotopes, and the source of the siderite was found to be aquifer cement rather than overburden nodules.

The second project is a pilot study designed to investigate the utility of Sr isotopes as a natural tracer of Marcellus Shale produced waters. Forty-one samples of produced water and one sample of hydraulic fracturing fluid were analyzed. Sr isotopic values were compared to previously analyzed values for western Pennsylvania AMD and shallower oil and gas brines, and were found to have a distinct isotopic signature. This distinction, along with the high concentrations of Sr in most Marcellus Shale produced waters, indicates that Sr isotopes constitute an extremely sensitive tracer of these waters.

In the third project, a four-step chemical sequential extraction procedure was carried out on drill cuttings from stratigraphic units above and below the Marcellus Shale, as well as on samples of the shale itself. Geochemical and Sr isotopic analyses of the leachates and dissolved samples suggest that there has been more than one generation of carbonate precipitation in the Marcellus Shale, as well as multiple stages of soluble salt dissolution and precipitation. Additionally, the water and ammonium acetate leaches had Sr isotopic values that fall within or just below the range previously measured for Marcellus Shale produced waters, indicating that the dissolved solids in the produced waters originate from within the shale itself.

2.0 STRONTIUM ISOTOPE QUANTIFICATION OF SIDERITE, BRINE, AND ACID MINE DRAINAGE CONTRIBUTIONS TO ABANDONED GAS WELL DISCHARGES IN THE APPALACHIAN PLATEAU

2.1 INTRODUCTION

The environmentally responsible production of energy resources such as shale gas requires the ability to characterize and monitor the interaction of fossil fuel-related fluids (e.g., coal mine discharges and waters associated with oil and gas production) with groundwater and environmentally important aquifers in order to identify contamination sources and delineate flow paths of affected waters (GWPC and ALL Cons., 2011). This is highlighted by the rapidly increasing pace of natural gas production from deep reservoirs in the Appalachian Basin, which has a long history of coal, oil, and gas extraction. Since 1859, over three million oil and gas wells have been drilled in the United States (Kharaka et al., 2003), with at least 325,000 in Pennsylvania alone (PA DEP, 2000). Unplugged or improperly plugged wells have been associated with stray gas migration and contamination of shallow aquifers from brine located in deep producing zones; their discharges have also been associated with stream pH as low as 3.5 (PA DEP, 2000, 2007).

In some areas of Pennsylvania, unplugged abandoned gas wells discharge sulfate-dominated high-TDS (total dissolved solids) water with >100 ppm iron; these discharges pollute receiving streams, contaminate soil, and destroy vegetation (Hedin et al., 2005). A common assumption is that these discharges originate from deep brines associated with Devonian gas-producing sands originally accessed by the wells. Dresel and Rose (2010) suggested that high iron concentrations reported in Pennsylvania oil and gas brines (e.g., Poth, 1962) could be contamination from the corrosion of steel casings in the wells from which they were sampled. Other work suggested that acid mine drainage (AMD) could be involved (Merritt and Emrich, 1970). In an analysis of 20 artesian discharges from abandoned wells in Clarion and Jefferson Counties, PA, Hedin et al. (2005) found chloride and sodium concentrations below 100 ppm, atypical of Pennsylvania oil and gas brines (Dresel and Rose, 2010; Poth, 1962). Although manganese and sulfate concentrations were similar to those found in local AMD, the discharges had higher concentrations of iron (40-215 mg/L), lower concentrations of aluminum (<1 mg/L) and silica (<10 mg/L), and generally higher pH (4.7-6.1). Hedin et al. (2005) suggested dissolution of siderite ($FeCO_3$), a carbonate mineral associated with coal-bearing Carboniferous units, could be involved. Here, we present the results of geochemical and strontium isotopic analyses of artesian gas well discharges in this region, uncontaminated well water from an associated aquifer, seeps from local surface mine spoil, Devonian brines, and iron carbonate from associated rocks in order to identify the sources of the groundwater contamination and to determine the surface and subsurface processes involved in its transport.

2.2 MATERIALS AND METHODS

2.2.1 Study area

The field area, in northeastern Clarion County, Pennsylvania, is located along the Leeper Anticline and Kane and Frills Corners Synclines in the Appalachian Plateau physiographic province (Figure 4); artesian flows are associated with synclinal areas (Leggette, 1936). Pennsylvanian Pottsville Formation sandstones form local aquifers. Surface mines of Allegheny Formation coals in this area are usually located on hilltops, and low-pH waters emanate at the toe of coal mine spoil piles. In the valleys, oil and gas wells tap units at depths from 200-400 m below the surface in the Upper Devonian Catskill sandstones of the Venango Group, which lie stratigraphically between the Bedford and Marcellus Shales, and have been a major source of oil, natural gas, and brines since the late 1800’s (Butts, 1906). Many of the wells, some over a century old, were abandoned without sealing; Pennsylvania still contains more than 8,500 unplugged oil and gas wells, over 200 of which are in Clarion County (PA DEP, 2000). Generalized stratigraphy and sample locations are shown in Figure 4.

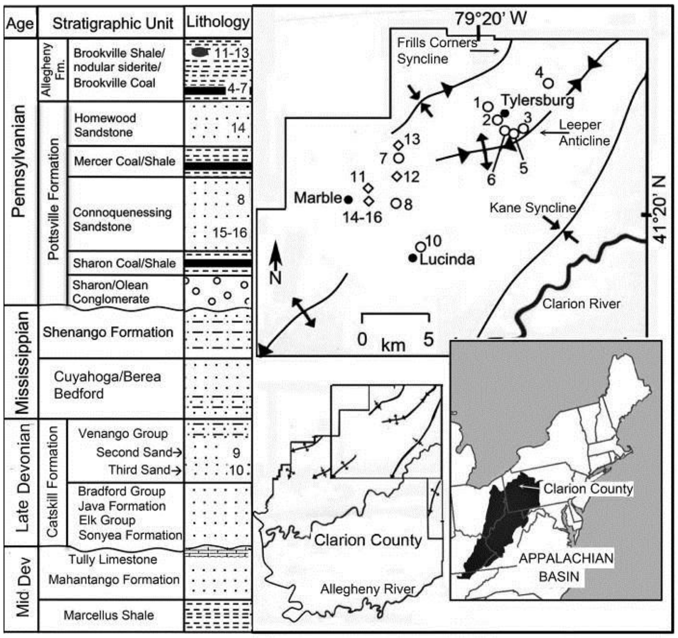

Figure 4. Left: Generalized stratigraphy of field area (modified from Milici and Swezey, 2006, and Shultz, 1999). Right: Structural geology of NE Clarion County showing location of siderite (diamonds) and fluid (circles) samples. Sample 9 (Timberline) is located approx. 35 km east of Tylersburg.

2.2.2 Water and rock samples

Water samples were collected between August 2009 and February 2010. The artesian gas well discharges (Licking wells, samples 1-3, Fig. 4) were taken from the openings of flowing abandoned natural gas wells (Fig. 5). Four low-pH water samples (#4-7, Fig. 4) were collected from mine spoil seeps near surface mines in the Brookville coal. Sample RN1 (#8, Fig. 4) was collected from a private drinking water well that taps the Connoquenessing Sandstone and represents groundwater unaffected by AMD, brine or contaminated gas well waters. Most residents in the area report that drinking wells drilled into the Connoquenessing are iron-contaminated; sample RN1 was from one of the only known wells in the area that produces drinkable water from this aquifer. Samples of Devonian brines were collected from Venango Group units: (1) Sample 9 (Timberline), produced water from a group of oil stripper wells that penetrate the Second Sand (~243 m depth) near Oil City, PA; and (2) Sample 10 (Ochs), from an active natural gas well that taps the Third Sand (~335 m depth) near Lucinda, PA.

Figure 5. Measuring flow from an artesian gas well, Clarion County, PA. A drainage pipe (pictured) was installed for accurate flow measurements.

Siliceous, siderite-containing buhrstone and septarian nodules originating from units overlying the mined Brookville coal seam were collected from mine spoil piles (samples 11-13, Figures 6 and 7; locations shown in Fig. 4). Samples of Pottsville Formation Homewood and Connoquenessing Sandstones (samples 14-16) were obtained as rock cuttings from a monitoring well (MW1; Fig. 8) that was drilled in 2006 to a depth of 135 m. Drilling was performed with an air rotary drill rig, and cuttings (Fig. 9) were collected in intervals ranging from <1 m to 6 m. The well penetrated units from the Pottsville Formation through the Cuyahoga Group. After drilling was completed, a borehole camera was inserted to a depth of 40 m, after which the danger of falling rocks prevented deeper filming. The camera identified water-producing zones at 11, 30, and 40 m, with production as high as 212 L/min in the deepest zone. These depths correspond to the Pottsville Formation Homewood and Connoquenessing Sandstone aquifers (Fig. 4).

Figure 6. Brookville coal mine spoil, where siderite Nodule 1 was collected.

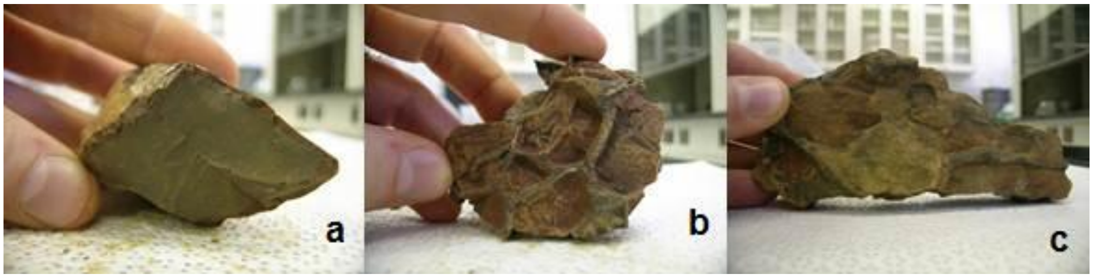

Figure 7. Siderite nodules: (a) Nodule 1; (b) septarian Nodule 2; (c) Nodule 3.

Figure 8. Measuring hydraulic head of monitoring well MW1.

Figure 9. Well cuttings from monitoring well MW1: (a) MW1-H48; (b) MW1-C105; (c) MW1-C128.

2.2.3 Analytical methods

Field measurements of water samples included pH, temperature, and alkalinity. Samples were filtered to 0.45 µm and aliquots for cation and isotopic analysis were acidified with ultrapure nitric acid (HNO_3) to a pH of <2.0; aliquots for anion analysis were refrigerated. Elemental concentrations for waters and dissolved solids were determined on a Spectroflame EOP ICP-AES, and anions were analyzed using a Dionex ICS-2000 ion chromatograph, both at University of Pittsburgh. Solid samples were crushed in a Ti-carbide ball mill, and iron concentrations for leachates of the solids were measured by G&C Coal Analysis Lab, Inc. Samples for X-ray diffraction (XRD) analysis were sieved to <45 μm and analyzed using a Phillips X'pert powder diffractometer with Cu Kα radiation at University of Pittsburgh. Peak positions (d-spacings) were determined using the Phillips X'pert Organizer software.

Crushed samples (2 g of well cuttings or 0.5 g of nodules) were leached with 1N ammonium acetate (buffered to pH 8) to remove exchangeable ions, followed by extraction of siderite with 10% ultrapure hydrochloric acid (HCl) for 24 h. Skousen et al. (1997) noted the low solubility of siderite associated with coal overburden rocks. Using ultrapure reagents, the method of Ellingboe and Wilson (1964), who reported <3% insoluble residue following a 24-hour extraction of siderite with 10% HCl, was followed. A 100% yield is not necessary because mass fractionation during dissolution reactions will have a negligible effect on the ^{87}Sr/^{86}Sr ratio of the siderite.

Petrographic and XRD analyses of rock cuttings from MW1 indicates that siderite occurs in the Pottsville Formation Homewood and Connoquenessing Sandstone aquifers as diagenetic cement between quartz and feldspar grains, an occurrence that is widely documented in sandstone units (e.g., Calvo et al., 2011; Karim et al., 2010, Morad, 1998). To assess the potential contribution of iron originating from the interaction of AMD-impacted groundwater with subsurface aquifers, XRD analysis was used to identify siderite in well cuttings from water-producing zones in the Pottsville formation (see discussion in 2.2.2). Cuttings from three of these zones were selected for chemical and isotopic analysis; one from the Homewood aquifer at a depth of 14.6-15.8 m (MW1-H48) and two from the deeper Connoquenessing aquifer, sample

MW1-C105, from 32.0-39.0 m depth, and sample MW1-C128, from a depth of 39.0-45.1 m. XRD traces for these samples are presented in Figure 10.

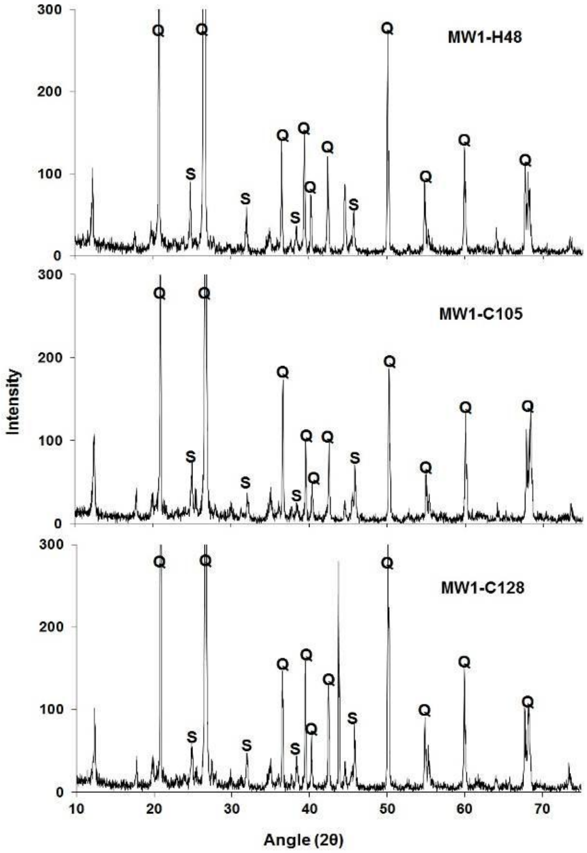

Figure 10. XRD traces of well cuttings of the Homewood (MW1-H48) and the Connoquenessing (MW1-C105; MW1-C128) aquifers from water-producing zones (14.6-15.8 and 32.0-45.1 m) indicate significant amounts of siderite (S) and quartz (Q).

Strontium isotope preparation and analysis was carried out under clean lab conditions at University of Pittsburgh. Aliquots containing approximately 2 µg Sr were evaporated to dryness and redissolved in 6N ultrapure HNO_3. Strontium in the samples was separated for isotopic analysis using Sr resin from Eichrom® in Teflon columns. The eluted Sr was evaporated to dryness and redissolved in 2N ultrapure HNO_3. An aliquot containing approximately 500ng Sr was evaporated onto a Re filament pre-loaded with a Ta oxide carrier agent. Strontium isotopes of the samples as well as the Sr standard SRM 987 were measured using a multidynamic method on a Finnigan MAT 262 thermal ionization mass spectrometer at University of Pittsburgh. Total procedural laboratory blank for sequentially extracted samples was 300 pg Sr. Our external reproducibility of $^{87}\mathrm{Sr}/^{86}\mathrm{Sr}$ is ±20 ppm. Our average $^{87}\mathrm{Sr}/^{86}\mathrm{Sr}$ for the Sr isotope standard SRM 987 during the time of these analyses was 0.710244 ±0.000015, corresponding to a seawater value of 0.709170.

Strontium isotope ratios are presented using $\varepsilon_{\mathrm{Sr}}^{\mathrm{SW}}$ (or $\varepsilon_{\mathrm{Sr}}$) notation, where the $^{87}\mathrm{Sr}/^{86}\mathrm{Sr}$ ratio of the sample is normalized to the globally uniform $^{87}\mathrm{Sr}/^{86}\mathrm{Sr}$ ratio of present-day seawater:

$$\varepsilon_{\mathrm{Sr}}^{\mathrm{SW}} = 10^4\left(\frac{^{87}\mathrm{Sr}/^{86}\mathrm{Sr}_{\mathrm{sample}}}{^{87}\mathrm{Sr}/^{86}\mathrm{Sr}_{\mathrm{seawater}}} - 1\right)$$

2.3 RESULTS

2.3.1 Geochemistry and mineralogy

Geochemistry for the fluid samples is reported in Table 1. The artesian gas well flows (#1-3) had similar pH (5.7-5.8) and alkalinity relative to the uncontaminated water well sample (#8), but elevated sulfate and iron concentrations (Table 1). The Venango oil and gas brines (#9 and 10) are high-TDS waters dominated by sodium (5,000-37,000 mg/L), chloride (13,000-72,000 mg/L), and calcium (1,500-9,000 mg/L); sample 10 also has comparatively high sulfate (387 mg/L). The low pH seeps (#4-7) contained sulfate (97-922 mg/L), silica (6-32 mg/L) and aluminum (5-39 mg/L) concentrations typical of AMD in Pennsylvania (Cravotta III, 2008;

Perry, 2001). The low iron concentrations of the seeps are likely the result of precipitation of iron minerals under oxidizing conditions within the mine spoil (Brady, 1998).

Table 1. Geochemistry of northwestern PA waters

Sample	pH	Temp	TDS	Alkalinity	Al	B	Ba	Ca	Fe	K	Mg	Mn	Na	Si	Sr	Cl	F	SO_4	Cations/ Anions
		(C)	(ppm)	(mg/L $CaCO_3$)	mg/L														(% Error)
Artesian gas well flows																			
1[a] Licking 15	5.8	NA[b]	711	37	<0.02	0.177	0.0133	80.8	130	4.98	66.3	10.4	5.59	5.70	0.392	3.90	0.24	716	-3.9
2 Licking 40	5.7	12	816	35	0.063	0.306	0.0119	90.8	180	5.35	73.3	12.4	4.96	6.18	0.314	7.20	0.32	862	-3.9
3 Licking 56	5.7	11	733	17	0.196	0.212	0.0049	87.3	157	4.82	75.8	10.5	3.15	5.75	0.209	2.96	2.0	741	3.6
Allegheny Formation coal mine seeps																			
4 LC45D	4.1	12	717	0	39.1	0.113	0.0111	98.8	2.91	3.71	98.8	12.8	2.90	31.8	0.227	8.50	7.6	922	-5.7
5 LS1	4.3	13	110	0	4.58	<0.08	0.0430	11.7	<0.1	1.06	11.2	1.49	3.38	6.11	0.0433	5.12	0.51	96.7	1.6
6 LS2	3.2	NA	440	0	29.4	0.099	0.0243	42.0	7.00	1.61	43.7	5.25	7.99	22.4	0.102	12.3	2.8	471	2.0
7 R64	4.3	NA	336	0	19.4	0.124	0.0148	30.1	0.321	5.90	34.5	5.58	3.62	21.4	0.106	10.4	6.9	374	-11
Pottsville Formation – unaffected aquifer																			
8 RN1	5.6	12	30	10	<0.02	<0.08	0.102	5.38	<0.1	1.18	4.3	<0.02	1.05	2.82	0.027	2.50	0.15	14.6	-0.90
Venango oil and gas brines																			
9 Timberline	NA	18	17,200	NA	0.026	0.451	96.5	1500	9.82	56.7	288	0.226	5340	3.77	24.9	13,100	<10	6.23	-5.6
10 Ochs	NA	10	111,000	NA	0.049	1.20	1.35	8980	2.42	112	1510	4.41	37,100	2.74	128	72,000	67	387	-3.3

[a] Sample numbers correspond to Figure 4.

[b] NA = not analyzed

Geochemistry of the siderite sample leachates is presented in Table 2. Manganese in siderite nodules and cement ranged from 0.6 to 1.4%. Potassium concentration in the siderite cement (1710-3980 ppm) was higher than that in the nodules (112-257 ppm). Al, Na, Si and K for one cement (MW1-H48) was anomalously high, possibly due to partial dissolution of alkali feldspar in the leaching process; however, the Sr isotopic composition of all three cements are similar to each other (within 4 ε_{Sr} units; Table 3) and distinct from the nodules. Nodule 1 had higher Ca, Mg, and Na, and lower Ba, Mn, Si, and S than Nodules 2 and 3. Even though Nodule 2 exhibited septarian characteristics (Fig. 7b), its geochemistry was not significantly different from that of Nodule 3. The main differences between Nodules 2 and 3 were in the concentrations of Ba and Si leached, both of which were higher in Nodule 3. Iron concentrations in the nodules ranged from 43.8 to 46.6%; in pure siderite, iron would make up 48.2%. Reported iron content of mined buhrstone and siderite nodules ranges from 25 to 45% (Harper and Ward, 1999, p. 29).

Table 2. Geochemistry of leached siderite samples

Sample	Al	B	Ba	Ca	Fe	K	Mg	Mn	Na	Si	Sr	S
					(mg/kg of rock leached)							
Allegheny Formation												
11[a] Nodule 1	2650	444	132	17,600	438,000	257	21,500	8390	378	240	56.0	176
12 Nodule 2 (septarian)	1610	476	2780	4640	440,000	151	4160	13,900	141	213	81.4	406
13 Nodule 3	1960	495	5320	3410	466,000	112	4940	13,900	137	529	48.0	333
Pottsville Formation aquifers												
14 MW1-H48 (Homewood aquifer)	36,800	662	234	12,800	478,000	3980	15,100	6300	359	5490	64.9	326
15 MW1-C105 (Connoquenessing aquifer)	7200	356	113	13,900	367,000	1510	17,800	7830	121	376	29.8	266
16 MW1-C128 (Connoquenessing aquifer)	7480	468	130	14,700	399,000	1710	16,100	10,900	115	235	34.3	252

[a] Sample numbers correspond to Figure 4.

XRD traces of the well cutting samples (MW1-H48, MW1-C105, and MW1-C128) show significant amounts of siderite and quartz (Fig. 10). Geochemistry of the leachates indicates that some Al, Ca, K, Mg, and Mn-bearing minerals are also present.

2.3.2 Strontium isotope geochemistry

Strontium isotope compositions for the waters and siderite are presented in Table 3. Strontium isotopic signatures can be used to identify and quantify sources of groundwater constituents as well as to characterize water-rock interaction in areas impacted by human activity (Banner et al., 1994; Brinck and Frost, 2007; Capo et al., 1998; Frost et al., 2002; Hamel et al., 2010). The relatively low Sr concentration and high ε_{Sr}^{SW} (0.03 ppm; +141) of unaffected groundwater (RN1) likely reflect a more radiogenic source of Sr from clay minerals and intercalated Paleozoic shales. The texture and relatively low ε_{Sr}^{SW} values (+11 to +21) of the siderite nodules are consistent with diagenetic formation in a marine environment. The low-pH mine seeps exhibit a wide range of ε_{Sr}^{SW} values and Fe concentrations (Fig. 11).

Table 3. Strontium isotope composition of northwestern PA waters and siderite samples

Sample	^{87}Sr/^{86}Sr	ε_{Sr}[c]
Waters		
Artesian gas well flows		
1[a] Licking 15	0.715587±10[b]	90.47±0.14
2 Licking 40	0.715864±10	94.38±0.14
3 Licking 56	0.716000±08	96.30±0.11
Allegheny Formation coal mine seeps		
4 LC45D	0.714503±11	75.19±0.16
5 LS1	0.717548±07	118.12±0.10
6 LS2	0.715697±10	92.02±0.14
7 R64	0.719102±08	140.04±0.11
Pottsville Formation – unaffected aquifer		
8 RN1 (Connoquenessing)	0.719159±07	140.84±0.10
Venango oil and gas brines		
9 Timberline	0.717338±09	115.16±0.13
10 Ochs	0.717022±16	110.71±0.23
Siderite		
Allegheny Formation		
11 Nodule 1	0.709972±08	11.29±0.11
12 Nodule 2 (septarian)	0.710502±14	18.77±0.20
13 Nodule 3	0.710651±11	20.87±0.26
Pottsville Formation aquifers		
14 MW1-H48 (Homewood)	0.715879±09	94.59±0.13
15 MW1-C105 (Connoquenessing)	0.716161±12	98.57±0.17
16 MW1-C128 (Connoquenessing)	0.715956±07	95.68±0.10

[a] Sample numbers correspond to Figure 4.

[b] 2σ uncertainty in last two digits of ^{87}Sr/^{86}Sr. Average ^{87}Sr/^{86}Sr during time of analyses was 0.710244, corresponding to a seawater value of 0.709170.

[c] $\varepsilon_{Sr} = (^{87}\mathrm{Sr}/^{86}\mathrm{Sr}_{sample}/^{87}\mathrm{Sr}/^{86}\mathrm{Sr}_{seawater} - 1)\bullet 10^4$; measured $^{87}\mathrm{Sr}/^{86}\mathrm{Sr}_{seawater}$ = 0.709170.

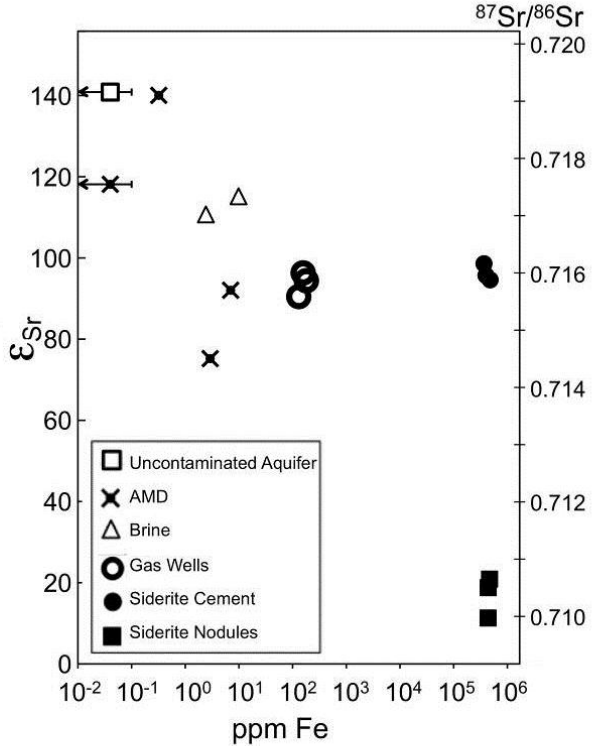

Figure 11. Strontium isotope compositions of samples plotted against iron concentration (mg/L for solutions; mg/kg for solids). Concentrations for the two lowest-Fe samples (aquifer RN1 and mine seep LS1; <0.1 mg/L) are indicated with the error bars.

Because it lies outside of the Licking Creek watershed, mine seep R64 is unlikely to be hydrologically related to the gas wells in this study. This is confirmed by its anomalous ε_{Sr} value (Table 3; Fig. 12a). However, it is an example of the range of AMD ε_{Sr} values that may be encountered within a relatively small area, emphasizing the need for site-specific analyses.

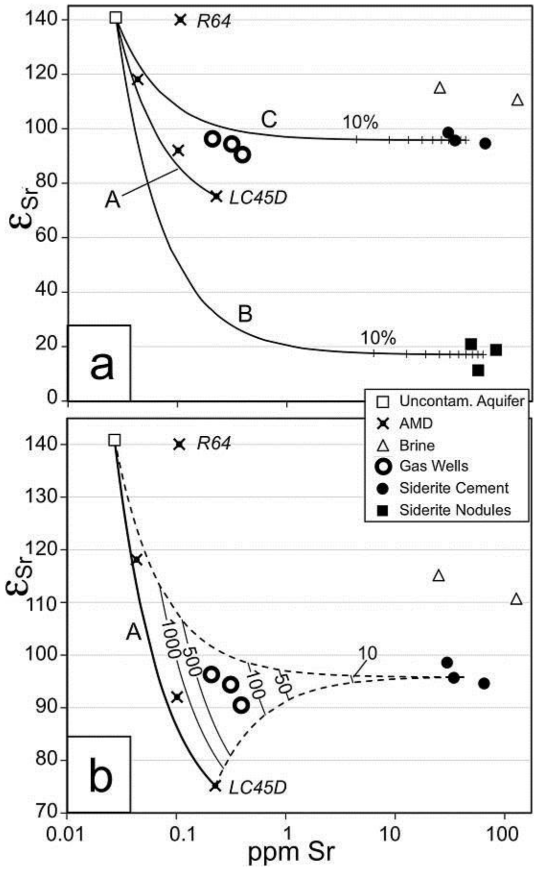

Figure 12. ε_{Sr} vs. Sr concentration (mg/L for solutions, mg/kg for solids). (a) Curve A shows a model mixing curve between RN1 and AMD seep LC45D, demonstrating the hydrologic connection of groundwater and the mine seeps. Curve B is a mineral dissolution model for mine spoil siderite dissolving in infiltrating groundwater, represented by RN1. Curve C is a mineral dissolution model for siderite cement in the aquifer dissolving into groundwater. Tick marks on curves B and C are calculated percentages of siderite dissolved into groundwater. (b) The mixing curve envelope between the range of groundwater/AMD compositions and siderite cement (dashed lines) clearly encompasses the gas well discharge values, suggesting that the Sr isotope composition of the gas well waters is controlled by dissolution of siderite cement in the aquifer. Labeled contours indicate the ratio of water+AMD to dissolved siderite.

The uncontaminated groundwater and remaining mine seeps have a range of ε_{Sr} values from +75 to +141. Figure 12 is a mixing diagram (ε_{Sr} vs. ppm Sr) for the mine seeps and uncontaminated aquifer sample RN1. The strong correlation indicates that these waters are hydrologically connected, with their strontium geochemistry controlled by mixing of groundwater, represented by sample RN1 from the only known unaffected well in the aquifer, with variable amounts of acid mine drainage.

The Sr isotopic compositions of the artesian gas well flows (ε_{Sr}^{SW} = +90 to +94) are distinct from the siderite nodules, uncontaminated groundwater, and the oil and gas brines (+111 and +115).

2.4 DISCUSSION

2.4.1 Sources of TDS to the artesian gas well discharges

Following surface mining, exhumation and oxidation of pyrite-bearing rocks releases dissolved iron, sulfate, and H^+ (Rose and Cravotta, 1998). Assuming that all of the sulfate in the AMD seeps studied here is a result of pyrite oxidation, approximately 70-90% of the iron from pyrite dissolution has precipitated out within the mine spoil (Brady, 1998); thus the seeps have iron concentrations that are insufficient to explain the high iron concentrations (130-180 mg/L) in the gas well flows.

The high iron content and intermediate ε_{Sr}^{SW} values of the gas well discharges (Fig. 11) could be explained by interaction of groundwater or AMD with siderite. The two possible sources of iron are nodules associated with surface mining and siderite cement in the aquifer.

2.4.2 Water-aquifer mixing models

Strontium can be considered a conservative element in most hydrologic systems, so the $^{87}Sr/^{86}Sr$ ratio of waters is a good indicator of fluid mixing and water-rock interaction (Banner et al., 1989). The ε_{Sr} values of the well discharges fall within the range for aquifer siderite, and between the values for uncontaminated groundwater and mine spoil siderite nodules (Fig. 11). To differentiate between these two possible siderite sources of Sr, mineral dissolution models (e.g., Uliana et al., 2007) were constructed using Sr concentrations and isotopic compositions of uncontaminated groundwater (RN1) and the two siderite endmembers. While sample RN1 may not be completely representative of unaffected groundwater, any "true" endmember is likely to fall along the AMD-groundwater mixing curve (Fig. 12a), perhaps extending it to slightly higher ε_{Sr} values. The choice of the "uncontaminated" groundwater endmember will not significantly affect the mineral dissolution models in this case.

Mineral dissolution model curves are shown in Figure 12a; the tick marks along curves B and C indicate increments of dissolved siderite required to shift the ε_{Sr} and Sr concentrations along the curves from the uncontaminated aquifer endmember. In both cases, the amount of siderite dissolution required to explain the gas well discharge data is small (<1% for siderite cement, <0.1% for siderite nodules). However, when Sr concentrations are considered, the models indicate that mine spoil siderite nodules are not a viable endmember to explain the gas well discharge values, as no conceivable mixing curves between groundwater (curve B) or any of the hydrologically connected mine seeps will intercept the well discharges.

In contrast, a mineral dissolution model curve between groundwater and aquifer siderite (curve C, Fig. 12a) lies near the gas well discharge values. When the rest of the hydrologically connected AMD seeps are considered as possible endmembers, it is clear that the gas well discharges fall well within the mixing envelope between likely water sources and siderite cement. Figure 12b shows a mineral dissolution model with the aquifer siderite cement mixing with the possible range of hydrologically-connected groundwater-AMD endmembers. The contours indicate the ratio of water to dissolved siderite in the mixtures. Both the Sr concentrations and ε_{Sr}^{SW} values in the gas well discharges can be explained by interacting the aquifer-AMD mixtures with dissolved siderite at a water/siderite ratio of 100-500 L/kg.

An additional possibility is that the gas well discharges represent a mixture of deeper brines with the AMD waters (e.g., seep LC45D, Fig. 12b). However, because the concentration of Sr in the brine is so much greater than that in the AMD ($Sr_{brine}/Sr_{AMD} = 10^2$ to 10^3), any variation in the brine/AMD ratio outside a narrow range of 0.002 to 0.004 would lead to large, easily distinguishable variations in gas well ε_{Sr}^{SW} values. Leakage of deep brines into groundwater + AMD is not likely to produce the uniform ε_{Sr}^{SW} values observed among the three potential brine sources (gas wells). In addition, this would not explain the relatively high iron concentrations of the gas well waters (Fig. 11). Iron carbonate cement within the aquifer sandstones provides the major source of dissolved iron and controls the strontium isotope composition in the gas well waters.

2.4.3 Processes involved in the generation of the contaminated artesian gas well discharges

The data indicate that both surface and subsurface processes are involved in generation of the contaminated gas well flows, and suggest the scenario shown in Figure 13. Following surface mining, the oxidation of pyrite in coal-related sedimentary rocks releases iron into waters that move through the mine spoil. Under near-surface oxidizing conditions, iron precipitates, lowering iron concentrations in the water and reducing pH (Brady, 1998). Bedding plane partings and stress-release fractures perpendicular to ridge tops related to Appalachian orogenic folding provide conduits into shallow (<60-70 m depth) aquifers (Winters and Capo, 2004;

Wyrick and Borchers, 1981). As acidic water migrates downward into the Homewood and Connoquenessing aquifers, dissolution of diagenetic siderite cement results in the release of iron. Although siderite is relatively insoluble compared to other carbonate minerals (Ellingboe and Wilson, 1964; Skousen et al. 1997), saturation indices for the gas well waters (Table 4) indicate that siderite is capable of dissolving under the acidic, reducing conditions that likely prevail within the aquifers (McMahon et al., 2009). As iron and sulfate-rich waters move through the aquifer, neutralization reactions cause an increase in pH.

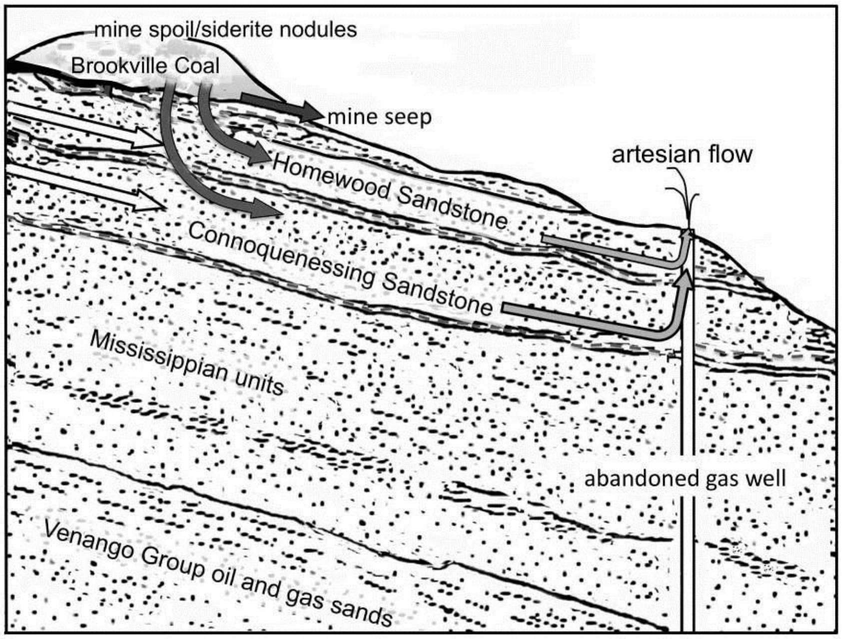

Figure 13. Generalized hydrogeologic cross-section (modified from Merritt and Emrich, 1970 and Hedin et al., 2005). AMD (dark gray arrows) infiltrates into shallow aquifers, dissolving siderite cement. Fractures and damaged well casings can act as conduits that bring the metal- and sulfate-contaminated waters to the surface via artesian flow.

Table 4. Saturation indices of northwestern PA waters determined by PHREEQc

Sample	pe	Albite $NaAlSi_3O_8$	$Fe(OH)_3$	Gibbsite $Al(OH)_3$	Goethite FeOOH	Hematite Fe_2O_3	Illite $(K,Mg,Al)Si_3O_{10}(OH)_2$	K-feldspar $KAlSi_3O_8$	K-mica $KAl_3Si_3O_{10}(OH)_2$	Kaolinite $Al_2Si_2O_5(OH)_4$	Siderite $FeCO_3$
Licking 15	-1	-7.0	-4.8	-0.73	0.59	3.1	-5.4	-4.6	-0.49	-0.37	-0.08
Licking 40	-1	-6.6	-5.0	-0.28	0.41	2.8	-4.3	-4.1	0.90	0.60	-0.10
Licking 56	-1	-8.2	-5.1	-1.6	0.31	2.6	-7.5	-5.5	-3.3	-2.1	-0.46
LC45D	8	-6.8	-2.6	-0.75	2.8	7.6	-4.7	-4.2	-0.13	1.1	–
	-1	-1.3	-7.4	3.4	-2.0	-2.0	6.3	1.3	13.6	9.3	–
LS2	8	-10.2	-4.8	-3.2	0.66	3.3	-12.2	-8.4	-9.3	-4.2	–
	-1	-1.1	-6.9	3.5	-1.4	-0.93	5.8	0.67	13.3	9.3	–
R64	8	-6.6	-2.8	-0.32	2.6	7.1	-4.1	-3.8	1.1	1.6	–
	-1	-1.9	-8.2	3.2	-2.8	-3.7	5.3	0.83	12.7	8.6	–

Most of the gas wells in the area were drilled before the 1984 Oil and Gas Act, which mandated stricter standards for well construction; compromised casings can allow overlying aquifer waters to enter wells and flow to the surface under artesian pressure. Upon reaching the surface, goethite and other iron minerals precipitate and pH drops. Similar infiltration of AMD into gas wells could be an explanation for high Fe concentrations observed by Dresel and Rose (2010) in many Appalachian Basin brines.

2.5 CONCLUSIONS

Artesian discharges of high-TDS water from some abandoned gas wells in the Appalachian Basin are not the result of transport of deep brine to the surface, but are caused by the infiltration of acidic, high-sulfate waters originating from shallow coal mines into underlying aquifers. These waters are modified by interaction with siderite cement, and are then transported to the surface via the gas wells. A common assumption that contaminated discharges from abandoned oil and gas wells originate from the upward migration of brine leads to the application of well plugging (Hedin et al., 2005). However, when shallow AMD is the primary source, this could divert contaminated water to other wells or fractures. In these cases the source of high TDS is not the original completion zone of the abandoned oil or gas well, and remediation must address the generation of AMD from surface mine spoils and potential pathways through shallow aquifers. Strontium isotopic analysis has the capability to differentiate between coal- and oil/gas-related inputs (e.g., shallow AMD, deep brines) into natural waters, and to distinguish between mineralogically identical but genetically different contaminant sources.

The combination of over a century of fossil fuel exploration and new drilling ventures such as the Marcellus Shale gas play presents unique challenges to the concurrent development of energy and water resources in the U.S. The storage of anthropogenic CO_2 in geologic formations in areas impacted by previous exploration activities will also require the ability to track movement of low-pH waters within confining and reservoir rock, quantify interaction of brine and groundwater, and identify the origin of contaminants detected during long-term monitoring (Monea et al., 2009; NETL, 2009). This work highlights the need to better understand the processes and migration pathways involved in water-rock interaction in developed areas. An approach that integrates geochemistry, hydrogeology and knowledge of historic mining and drilling activity is critical to the successful remediation of existing water quality problems and the protection of water resources in the Appalachian Basin and other geologically and hydrochemically complex areas.

3.0 GEOCHEMICAL AND STRONTIUM ISOTOPE CHARACTERIZATION OF PRODUCED WATERS FROM MARCELLUS SHALE NATURAL GAS EXTRACTION

3.1 INTRODUCTION

Development of the Appalachian Basin Marcellus Shale, one of the world's largest natural gas plays, has increased dramatically with the application of horizontal drilling and hydrofracturing, a process that uses 8-15 million liters of water for each well (Kerr, 2010; PA DEP, 2010). Waters produced from the well comprise a portion of the fracturing fluid, an injected water solution including various chemicals used to facilitate hydraulic fracturing, along with possible formation brines. These waters have total dissolved solid (TDS) contents often exceeding 200,000 mg/L, with elevated levels of Sr, Br, Na, Ca, Ba, and Cl, most likely from interaction with the producing shale formation (Keister, 2010). Currently, TDS is considered an EPA secondary drinking water contaminant at levels above 500 mg/L.

Deep injection is the least expensive method for disposing of produced water, with most produced water in the U.S. being disposed of in Class II injection wells that target formations with suitable porosity, permeability, and capacity (U.S. EPA, 2011). Unfortunately, only limited opportunities for deep injection exist in the areas of Pennsylvania where Marcellus Shale gas development is most intense (GWPC and ALL Cons., 2009). In these areas, increasingly greater volumes of produced water are being reused to hydraulically fracture subsequent wells. Where reuse is not practical, produced water is either treated for surface discharge or transported to nearby states where deep injection capacity exists (GWPC and ALL Cons., 2009). The storage and transportation of produced water prior to reuse, treatment, or deep injection provides some opportunity for these waters to become commingled with surface water or shallow groundwater through spills or releases. Deeper groundwater also could be affected if the integrity of the well is compromised (Kargbo et al., 2010).

Recent stream contamination events and produced water releases have highlighted the need for methods to distinguish between possible sources of TDS, such as fluids related to coal vs. oil/gas extraction. For example, in 2008, high levels of sulfate, chloride, and bromide-dominated TDS were measured in the Monongahela River in Pennsylvania (Renner, 2009a); the source of this contamination was determined to be outflows from wastewater treatment plants which process both coal mine water and Marcellus Shale produced water (PA DEP, 2009). Similarly, in 2009 a significant fish kill occurred in Dunkard Creek, a tributary of the Monongahela River that flows along the border between Greene County, PA, and Monongalia County, WV. This event was caused by a release of high-TDS water, the source of which is still under debate (PFBC, 2011; Renner, 2009b; Reynolds, 2009). Additionally, a number of fracturing fluid, produced water, and brine releases have occurred at Marcellus Shale well pads, including three releases at a single pad in Susquehanna County, PA, in which fracturing fluid reached a tributary of Towanda Creek (NYSDEC, 2011).

Whereas typical Marcellus Shale produced waters are chemically distinct from streams and uncontaminated groundwater, few geochemical parameters can unambiguously distinguish between all possible sources in the event of a spill or leakage. In Pennsylvania, such sources may include abandoned mine drainage, fly ash impoundments, brines from abandoned oil and gas wells targeting formations shallower than the Marcellus, road salt, wastewater outflows and septic systems, and industrial discharges. Here, strontium isotope ratios are applied to address these issues.

The isotopic ratio of radiogenic strontium-87 (^{87}Sr, produced by the decay of ^{87}Rb over geologic time) to the stable strontium isotopes ^{84}Sr, ^{86}Sr, and ^{88}Sr has been shown to be an effective tracer of water-rock interactions and has been used to identify and quantify sources of groundwater constituents in areas impacted by human activity (Banner et al., 1994; Bayless et al., 2004; Brinck and Frost, 2007; Christian et al., 2011; Hamel et al., 2010; Jiang et al., 2009; Leung and Jiao, 2006; Millot et al., 2011; Peterman et al., 2010). Unlike stable isotopes of oxygen, hydrogen and carbon, the isotope composition of strontium is not affected by evaporation (e.g., from holding ponds) or biological activity. In order for the isotope ratio of strontium (expressed as ^{87}Sr/^{86}Sr) to be used successfully as a natural tracer in ground and surface waters, the isotope ratios of the potential endmembers must be distinct. If potential endmembers have distinct strontium isotopic ratios, strontium isotopes can be used to sensitively detect of even minute amounts of contamination from brines, and potentially to identify waters interacting with rocks from specific stratigraphic units (Chapman et al., in prep).

In addition, understanding the sources of these high salts and metals may be useful in designing drilling strategies and understanding heterogeneities in the shale unit. Many formation brines, including those of the Appalachian Basin, have been found to have a significant component of evaporated seawater (Rowan, 2011; Rowan and De Marsily, 2001; Stueber and Walter, 1991). Conversely, the presence of lenticular salt deposits in a Marcellus core has led to the hypothesis that the high salinity originates from autochthonous salts (Blauch et al., 2009). Strontium isotopes can also be used to understand the origin of salts in produced waters (i.e., to determine if salts are from evaporated seawater and to identify additional sources of dissolved constituents such as carbonates or exchangeable sites on clays). An isotope study of Marcellus produced waters was carried out to (1) identify unique isotope “fingerprints” of Marcellus waters to aid in verification of safe disposal; and (2) determine the source of dissolved salts that are abundant and ubiquitous in Marcellus waters.

3.2 MATERIALS AND METHODS

3.2.1 Marcellus produced waters

Samples of hydrofracturing fluid and waters produced during and after drilling were obtained from wellheads and impoundments from four counties across Pennsylvania (Table 5; Fig. 14). Some were collected as time series from the start of pumping, and others from impoundments where they were being held prior to recycling or disposal. Samples BR-A1 through A5 were produced waters collected from five wells in Bradford County; samples BR-A3 through A5 had been recycled through several fracturing operations. Samples beginning with WE were collected from two closely spaced wells (<1 km apart; designated by ‘A’ and ‘B’ in sample name) in Westmoreland County, at the indicated number of days after hydrofracturing. Samples WA-BA-4 through 10 were collected in Washington County from three different wastewater impoundments, at various depths below the water surface (Table 5). Samples WA-A11 through A30 were collected from a well in Washington County at the indicated number of days after hydrofracturing. Samples beginning with GR were collected from a well in Greene County at the indicated number of days after hydrofracturing; GR-AF is a sample of the water used to hydrofracture that well (hydrofracturing fluid).

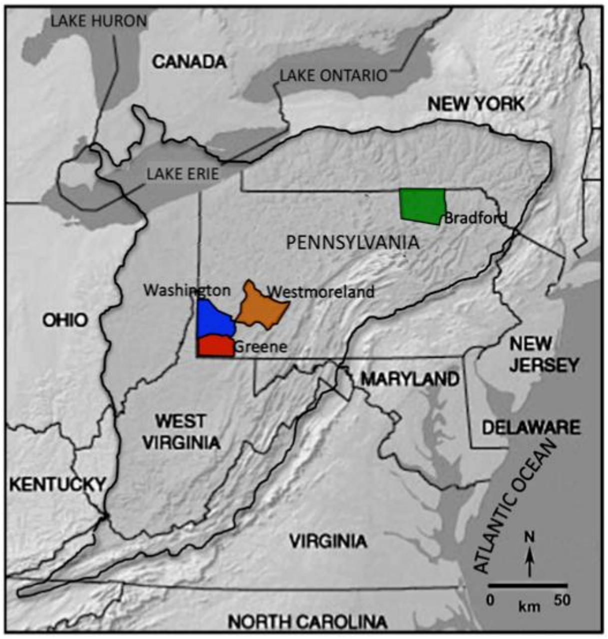

Figure 14. Location map of Marcellus Shale and counties where produced water was collected.

Table 5. Major element and strontium isotope data for Marcellus produced water samples

Sample/Loc.	Description	Na	Mg	Ca	Fe	Sr	Ba	Cl	SO_4	TDS	$^{87}Sr/^{86}Sr^a$	$\varepsilon_{Sr}{}^b$
		mg/L								g/L		
Bradford Co., PA												
BR-A1	Produced water	30,400	538	6,120	117	1,970	5,490	77,065	NA[c]	109.5	0.710653 ± 07	20.91 ± 0.10
BR-A2	Produced water	49,400	1,750	20,800	123	5,230	12,000	159,126	NA	211.4	0.710270 ± 10	15.51 ± 0.14
BR-A3	Recycled produced water	41,900	1,110	11,300	73.7	3,340	7,820	68,303	NA	154.1	0.710742 ± 06	22.17 ± 0.08
BR-A4	Recycled produced water	34,000	840	7,930	50.5	2,870	6,470	169,617	NA	136.6	0.710757 ± 08	22.38 ± 0.11
BR-A5	Recycled produced water	27,600	726	7,050	55.3	2,600	5,860	72,545	NA	120.9	0.710733 ± 09	22.04 ± 0.13
Greene Co., PA												
GR-AF	Fracturing fluid	20,923	567	4,377	16.0	1,389	393	41,851	186	88.74	0.710084 ± 08	12.89 ± 0.11
GR-A1	Produced water, day 1	26,020	776	6,532	43.7	1,397	1,108	63,700	111	127.2	0.710988 ± 08	25.64 ± 0.11
GR-A2	Produced water, day 2	30,100	828	7,903	44.9	1,823	1,560	65,000	123	138.8	0.710976 ± 10	25.47 ± 0.14
GR-A3	Produced water, day 3	26,840	866	7,372	49.2	1,721	1,487	67,300	130	137.8	0.710957 ± 07	25.20 ± 0.10
GR-A4	Produced water, day 4	30,910	755	8,874	38.1	2,009	1,756	70,200	94	146.2	0.710961 ± 09	25.25 ± 0.13
GR-A5	Produced water, day 5	28,270	762	7,952	1.10	1,868	1,638	71,200	93	143.1	0.710975 ± 08	25.45 ± 0.11
GR-A7	Produced water, day 7	32,800	841	8,786	26.6	2,415	962	81,900	118	157.0	0.710148 ± 08	13.79 ± 0.11
GR-A15	Produced water, day 15	32,380	953	9,634	28.1	2,275	2,273	86,500	128	161.5	0.711160 ± 09	28.06 ± 0.13
GR-A20	Produced water, day 20	34,520	976	10,390	36.1	2,484	2,525	87,700	133	188.2	0.711173 ± 09	28.24 ± 0.13
GR-A27	Produced water, day 27	NA	NA	NA	NA	NA	NA	NA	NA	NA	0.711183 ± 41	28.39 ± 0.58

Table 5 cont.

Washington Co., PA												
WA-A11	Produced water, day 11	32,500	1,267	12,278	38.6	1,393	151	88,503	NA	136.2	0.711129 ± 08	27.62 ± 0.11
WA-A13	Produced water, day 13	35,070	1,478	14,028	41.8	1,694	194	102,122	NA	146.7	0.710988 ± 10	25.64 ± 0.14
WA-A15	Produced water, day 15	37,100	1,632	15,269	17.3	1,832	253	107,315	NA	153.4	NA	
WA-A17	Produced water, day 17	38,530	1,671	15,875	21.6	1,872	296	102,605	NA	156.7	0.711056 ± 11	26.59 ± 0.16
WA-A20	Produced water, day 20	40,350	1,820	16,509	19.0	1,888	328	115,278	NA	167.8	0.711088 ± 09	27.05 ± 0.13
WA-A25	Produced water, day 25	46,260	1,896	17,612	15.6	2,045	349	116,069	NA	168.4	0.711021 ± 10	26.10 ± 0.14
WA-A30	Produced water, day 30	47,881	1,992	18,080	NA	2,151	379	NA	NA	169.4	0.711076 ± 08	26.88 ± 0.11
WA-B1-8	Impoundment #1, 8' depth	20,310	880	8,682	18.7	1,192	176	59,600	129	108.0	0.710880 ± 10	24.11 ± 0.14
WA-B1-4	Impoundment #1, 4' depth	20,440	890	8,796	15.8	1,205	191	65,300	NA	117.0	0.710905 ± 10	24.47 ± 0.14
WA-B2-9	Impoundment #2, 9' depth	20,510	859	8,779	5.12	1,277	389	59,400	NA	110.7	0.710969 ± 08	25.37 ± 0.11
WA-B2-6	Impoundment #2, 6' depth	20,910	866	8,818	4.37	1,296	339	58,700	NA	108.0	0.710954 ± 10	25.16 ± 0.14
WA-B3-10	Impoundment #3, 10' depth	12,890	570	5,674	0.067	795	10.5	36,700	122	71.37	0.710737 ± 10	22.10 ± 0.14
WA-B3-5	Impoundment #3, 5' depth	12,940	589	5,733	0.066	803	9.54	36,800	95	71.44	0.710722 ± 09	21.88 ± 0.13
Westmoreland Co., PA												
WE-A1.5	Produced water, day 1.5	NA	NA	349	NA	46.0	70.0	NA	NA	14.84	0.711992 ± 06	39.79 ± 0.08
WE-A2	Produced water, day 2	2,792	43	624	NA	88.0	179	10,315	29	21.41	0.712013 ± 10	40.09 ± 0.14
WE-A4	Produced water, day 4	11,747	217	2,278	NA	381	740	28,979	8.4	44.84	0.712036 ± 10	40.41 ± 0.14
WE-A5	Produced water, day 5	14,216	254	2,880	NA	450	888	32,190	8.2	51.11	0.712027 ± 10	40.29 ± 0.14
WE-A7	Produced water, day 7	18,288	381	3,938	NA	651	1,405	42,099	5.9	65.72	0.712044 ± 06	40.53 ± 0.08
WE-A12	Produced water, day 12	23,928	518	5,603	NA	934	2,193	47,885	4.2	81.17	0.712013 ± 08	40.09 ± 0.11
WE-A15	Produced water, day 15	24,820	629	6,292	NA	1,127	2,687	53,458	4.2	89.53	0.712019 ± 10	40.17 ± 0.14
WE-A29	Produced water, day 29	26,297	671	6,236	NA	1,215	2,987	76,581	2.2	99.03	0.712091 ± 07	41.19 ± 0.10
WE-B3	Produced water, day 3	9,901	694	1,239	NA	214	333	19,026	NA	33.31	0.712076 ± 11	40.98 ± 0.16
WE-B5	Produced water, day 5	16,704	376	2,782	NA	533	1,058	30,640	NA	55.56	0.712108 ± 07	41.43 ± 0.10
WE-B7	Produced water, day 7	18,288	490	3,900	NA	738	1,490	40,710	NA	69.42	0.712088 ± 08	41.15 ± 0.11
WE-B9	Produced water, day 9	18,510	559	4,627	NA	900	1,892	46,756	NA	78.39	0.712108 ± 08	41.43 ± 0.11
WE-B13	Produced water, day 13	22,437	211	5,749	NA	1,063	2,306	71,117	NA	89.25	0.712117 ± 09	41.56 ± 0.13
WE-B18	Produced water, day 18	NA	NA	6,278	NA	1,380	2,700	NA	NA	98.07	0.712113 ± 09	41.50 ± 0.13

[a] Uncertainty in last two decimal places of ^{87}Sr/^{86}Sr ratio.

[b] $\varepsilon_{Sr} = (^{87}Sr/^{86}Sr_{sample}/^{87}Sr/^{86}Sr_{seawater} - 1)\bullet 10^{4}$; measured $^{87}Sr/^{86}Sr_{seawater}$ = 0.709170.

[c] NA = not analyzed

3.2.2 Coal mine drainage

Samples of coal mine drainage (acid, circumneutral and net alkaline) from bituminous coals of the Pittsburgh and Allegheny Formations (Pittsburgh, Freeport, Kittanning, Clarion, and Brookville) were analyzed for Sr isotopes to compare with potential Marcellus produced water. Major element and Sr isotope geochemistry is presented in Table 6.

Table 6. Major element and strontium isotope data for coal mine discharges in western Pennsylvania

Discharge	Coal seam	Date sampled	Na	Ca	Mg	Fe	Sr	Cl	SO_4	pH	Alkalinity g $CaCO_3$	$^{87}Sr/^{86}Sr$	ε_{Sr}
			- - - - - - - - mg/L	- - - -	- - - -	- - - -	- - - -	- - - -	- - - -				
Monongahela Group -Pittsburgh Formation													
Douglas Run	Pittsburgh	26-Feb-98	222	79	27.4	16.7		65	461	6.7	279		
		3-Mar-99	222	85	27.5	13.1	1.6	122	410	6.4	304	0.712212 ± 10	42.90 ± 0.14
		14-Jul-99	204	79	26.6	18.4	1.3	97	428	6.0	278	0.712224 ± 13	43.06 ± 0.18
Lowber (Marchand)	Pittsburgh	26-Feb-98	481	153	44.0	79.0		78	1332	6.3	320		
		3-Mar-99	483	163	42.4	78.3	2.6	97	1330	6.1	332	*0.712568* ± 76	47.92 ± 1.07
		14-Jul-99	426	149	40.8	75.0	1.9	56	1315	6.0	360		
		22-Feb-01										0.712530 ± 13	47.38 ± 0.18
Guffey-Upper	Pittsburgh	26-Feb-98	257	65	21.6	33.0		46	570	6.2	224		
		14-Jul-99	281	51	16.0	21.5	1.1	78	464	6.2	350	0.712195 ± 10	42.66 ± 0.14
Guffey-Lower	Pittsburgh	26-Feb-98	191	62	21.0	26.4		58	407	6.3	211		
		6-Mar-99	235	66	20.1	22.0	1.4		456	6.3		0.712120 ± 09	41.60 ± 0.13
		14-Jul-99	133	61	20.9	23.6	1.2	81	285	6.0	192	0.712229 ± 09	43.13 ± 0.13
Irwin upper	Pittsburgh	26-Feb-98	172	111	30.7	56.0		57	782	6.0	109		
		3-Mar-99	125	122	34.7	70.4	1.6	66	715	6.0	109	0.712622 ± 11	48.68 ± 0.16
		14-Jul-99	137	107	32.3	62.1	1.2	70	590	7.0	132	0.712611 ± 09	48.52 ± 0.13
		22-Feb-01										0.712601 ± 09	48.38 ± 0.13
Coal Run	Pittsburgh	26-Feb-98	115	78	26.7	17.3		86	369	6.2	128		
		3-Mar-99	83	78	28.0	16.0	1.5	87	298	5.8	121	0.712364 ± 09	45.04 ± 0.13
		14-Jul-99	91	75	26.4	18.7	1.1	86	306	6.2	148	*0.712367* ± 49	45.08 ± 0.69
		22-Feb-01										0.712366 ± 11	45.07 ± 0.16
Export-artesian	Pittsburgh	3-Mar-99	19	101	33.5	1.3	0.7	49	545	2.8	0	0.712421 ± 10	45.84 ± 0.14
		14-Jul-99	22	107	38.3	1.5	0.7	13	599	3.2	0	0.712399 ± 09	45.53 ± 0.13
		22-Feb-01										0.712365 ± 10	45.05 ± 0.14
Delmont, lg.	Pittsburgh	26-Feb-98	30	88	28.4	31.0		21	491	5.0	13		
		3-Mar-99	23	82	27.0	38.3	0.7	22	404	3.4	0	*0.712522* ± 46	47.27 ± 0.65
		14-Jul-99	23	86	27.6	31.2	0.6	30	375	5.2	22	0.712596 ± 10	48.31 ± 0.14
		22-Feb-01										0.712638 ± 10	48.90 ± 0.14
Yough waterfall	Pittsburgh	3-Jul-09										0.712096 ± 12	41.26 ± 0.17
Scrubgrass	Pittsburgh	19-Oct-99	291	106	36.4	81.8	1.6	279	601	6.1	160		
		15-Feb-01					1.7	294		6.3	171	0.711730 ± 12	36.10 ± 0.17
		17-Mar-01										0.711675 ± 14	35.32 ± 0.20
		25-Jan-02	256	106	38.1	80.5	1.5		550	6.1	159		
		28-Feb-02	242	98	33.0	64.2	1.4		564	6.2	209		
		21-Mar-02	263	109	37.8	66.8	1.4		548	6.1	164		

Table 6 cont.

Allegheny Formation

Fawn #91	Freeport	22-Feb-01						8		3.2	0	0.712288 ± 09	43.97 ± 0.13
Penn-Allegheny	Freeport	22-Feb-01	577	168	39.3	76.6	3.1	60		6.8	444	0.712266 ± 11	43.66 ± 0.16
Keystone	Freeport	17-Jun-99	84	49	13.3	26.9	1.2	11	276	6.6	130	0.712573 ± 12	47.99 ± 0.17
Waterman	Freeport	17-Jun-99	16	120	33.6	9.7	0.7	6	491	4.1	0	0.714174 ± 13	70.56 ± 0.18
Bird	U/L Kittanning	17-Jun-99	121	200	63.7	75.1	0.8	18	1013	6.0	86	0.713888 ± 15	66.53 ± 0.21
Jennings/raw	M Kittanning	26-Jan-01	3	113	68.9	79.9	0.3	20		3.2	0	0.713158 ± 11	56.23 ± 0.16
Jennings/PITI			3	115	69.6	80.0							
DeSalle II	M Kittanning	26-Jan-01	6	185	179.9	32.8	0.3	1		2.8	0	0.714687 ± 14	77.80 ± 0.20
Oven Run E	L. KittanningRaw AMD	15-Oct-99	6	183	111.4	22.5		3	1060	2.9	0		
Howe Bridge	Clarion	09-Jul-99	10	190	105.7	240.1	0.8	6	1151	6.6	169		
		25-Jan-01	15	205	88.0	95.1	1.0	4		6.1	39	0.715996 ± 12	96.25 ± 0.17
Filson	Clarion	09-Jul-99	6	182	43.2	47.7	0.3	19	392	6.4	356		
		19-Nov-99	8	64	40.9	53.4		19	354	5.6	61		
			8	63	46.1	53.1							
		25-Jan-01	8	173	44.6	44.2	0.2	3		5.1	50	0.716260 ± 09	99.98 ± 0.13
Strattanville	Clarion	09-Jul-99	7	149	236.3	385.4	0.2	4	2136	4.4	0	0.718181 ± 14	127.06 ± 0.20
Morrison	Clarion	09-Jul-99	10	239	123.5	202.8	0.5	4	1121	6.2	323		
LC-45D seep	Brookville	1-Aug-09	2.9	98.80	99	2.9	0.2	9	922[a]	4.1	0	0.717548 ± 11	118.14 ± 0.16
LS-2 seep	Brookville	1-Feb-10	8.0	42.00	44	7.0	0.1	12	471[a]	3.2	0	0.714503 ± 10	75.20 ± 0.10
R64	Brookville	1-Aug-09	4	30	34.5	0.3	0.1	10	374[a]	4.3	0	0.719102 ± 08	140.05 ± 0.11
BC-2-MW-1 (mine pool)	Brookville	26-Apr-10				5.2	0.3		25[a]	7.4	164	0.712912 ± 17	52.77 ± 0.24
BC-6-NBG-15 (seep)	Brookville	26-Apr-10				62.8	0.1		321[a]	3.2	0	0.716131 ± 14	98.16 ± 0.20

[a] Determined by ion chromatography; all other sulfate values determined by ICP-AES from S concentrations.

3.2.3 Analytical methods

Samples were filtered to <0.45 µm and acidified with ultrapure concentrated nitric acid (HNO_3). Major and trace elements were analyzed by ICP-MS and ICP-OES at DOE-NETL Pittsburgh, Bucknell University, and University of Pittsburgh. Strontium isotope preparation and analysis were carried out under clean lab conditions at University of Pittsburgh. Using Sr concentrations determined by ICP-OES, aliquots containing between 2 and 10 µg Sr were evaporated to dryness, redissolved in 6N ultrapure HNO_3, and eluted through columns containing Eichrom® Sr resin to separate Sr from all other constituents in the sample. The eluted Sr was evaporated to dryness and redissolved in 2N ultrapure HNO_3. An aliquot containing approximately 500 ng Sr was evaporated onto a Re filament pre-loaded with a Ta oxide carrier agent. Strontium isotopes of the samples as well as the Sr standard SRM 987 were measured using a multidynamic method on a Finnigan MAT 262 thermal ionization mass spectrometer. The average $^{87}Sr/^{86}Sr$ ratio of SRM 987 over the period of these analyses was 0.710244, with an estimated external reproducibility of ±0.000015.

Strontium isotope ratios are presented using ε_{Sr}^{SW} (or ε_{Sr}) notation, where the $^{87}Sr/^{86}Sr$ ratio of the sample is normalized to the globally uniform $^{87}Sr/^{86}Sr$ ratio of present-day seawater:

$$\varepsilon_{Sr}^{SW} = 10^4 \left(\frac{^{87}Sr/^{86}Sr_{sample}}{^{87}Sr/^{86}Sr_{seawater}} - 1 \right)$$

Our measured seawater $^{87}Sr/^{86}Sr$ value is 0.709170.

3.3 RESULTS

3.3.1 Produced water dissolved load

Major element data from the Pennsylvania produced waters reported here (Table 5) indicate that these waters share many of the characteristics previously reported for Marcellus Shale produced waters (Blauch et al., 2009), including variable but generally high TDS (20,000 to >200,000 mg/L), a predominance of sodium and chloride in the dissolved load, and very high concentrations of barium and strontium (up to 12,000 and 5,200 mg/L, respectively). Chloride is largely balanced by Na^+, with Ca^{2+} providing most of the remaining charge balance (Fig. 15a). The wells and impoundment waters from Washington County (circles in Fig. 15a) have more calcium-rich compositions compared to the other produced waters. Comparison of sodium and calcium to the sum of all cations (Fig. 15b) indicates the importance of Na and Ca to the overall dissolved load. The offset of the Bradford County samples from this trend reflects the extremely high concentrations of Sr and Ba in these waters, which contribute significantly to the overall dissolved load. There are no clear geographic trends in concentration from the southwestern-most to the northeastern-most produced waters, although the Bradford County produced waters tend to have the highest concentrations of dissolved constituents, and the Westmoreland County waters the lowest.

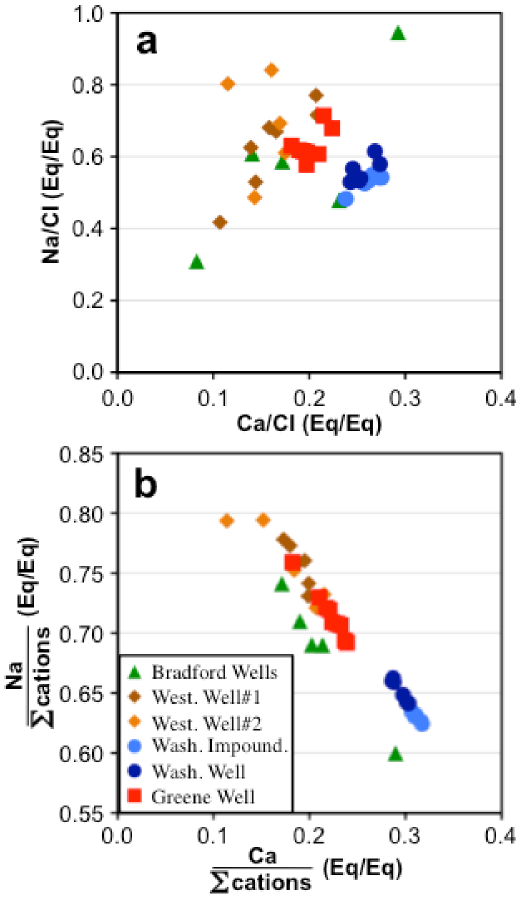

Figure 15. Variations in the chemical composition of Marcellus Shale produced water. (a) Sodium/chloride ratios plotted against calcium/chloride on an equivalent basis. Na and Ca are the dominant cations that together account for most of the Cl^- produced waters, suggesting a source with both NaCl- and $CaCl_2$-type salts or brines. (b) Sodium and calcium normalized to the sum of all cations, on an equivalent basis. The offset of the Bradford County samples (green triangles) from the rest of the trend reflects the very high Ba and Sr content of these waters.

Marcellus Shale gas well produced waters are known for their high Ba and Sr concentrations (Blauch et al., 2009). Both of these are alkaline earth elements, with geochemical characteristics similar to those of calcium. When normalized to calcium to account for the large variations in TDS, Ba and Sr show a positive correlation across the region, with only the Greene County well data diverging significantly from the trend (Fig. 16a), However, data from each well or region fall within unique, non-overlapping parts of this plot. In contrast, the Mg/Ca ratio shows no systematic correlation with Sr/Ca in the Marcellus Basin as a whole, although individual wells or regions sometimes have a weak correlation (Fig. 16b). In addition, the Mg/Ca ratio varies over a much smaller range of values (most within the molar ratio of 0.10-0.15) compared to the range of Ba/Ca and Sr/Ca ratios. Thus Mg and Ca appear to be coupled in their behavior across the basin, whereas Ba, and to a lesser extent Sr, are affected more strongly by local variations.

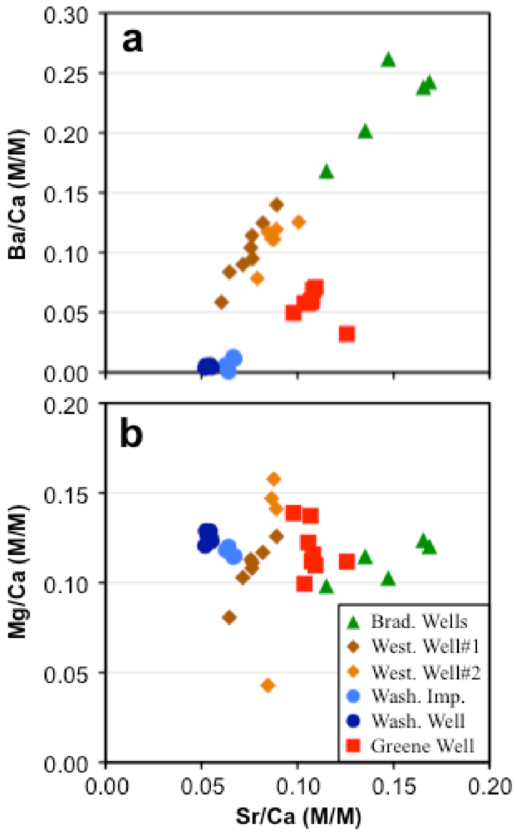

Figure 16. Variations in strontium, barium and magnesium with calcium in Marcellus Shale produced waters. (a) Ca-normalized Ba concentrations show a generally coherent positive trend across Pennsylvania when plotted against Ca-normalized Sr, with the well waters from Greene County showing the most significant deviation from the trend. (b) Ca-normalized Mg concentrations do not exhibit a regional-scale trend, and are only weakly correlated within each well or region.

The shifts in Ba and Sr across the basin are unlikely to result solely from variations in the shale barite content (and dissolution in hydraulic fracturing fluid), as the Sr/Ba ratios in the produced waters are significantly higher than those expected for marine barite (0.03-0.08; Paytan et al., 2007). The positive correlations of barium with strontium at high Sr/Ba ratios within individual wells argues against either introduction of Ba from drilling muds or removal of Ba by scaling (e.g., precipitation of $BaSO_4$ in pipes and pore spaces) prior to extraction of the brine, as both of these should affect Ba much more strongly than Sr. The range of barium and strontium concentrations in produced waters is most likely controlled by the combined dissolution of Ba- and Sr-rich minerals such as barite, celestite, and strontianite, with the large differences in Ba/Ca and Sr/Ca among different regions reflecting the co-occurrence of these minerals at different abundances within the Marcellus Shale.

3.3.2 Sr isotope composition of produced waters

Strontium isotope ratios for Marcellus Shale produced waters are reported in Table 5. Most produced waters fall within an ε_{Sr} range of +13.8 to +28.4 ($^{87}Sr/^{86}Sr$ = 0.71015-0.71118); only the Westmoreland County wells deviate significantly, with an ε_{Sr} range of +39.8 to +41.6 ($^{87}Sr/^{86}Sr$ = 0.71199-0.71212). The total range of values for Marcellus Shale produced waters, including the Westmoreland County samples, is quite restricted compared to possible water and rock with which they might interact. For example, Phanerozoic marine limestone falls within a range of -35 to 0 (Burke et al., 1982), and abandoned coal mine drainage outflows in western Pennsylvania can range from +35 to +140 (Table 6). Assuming that this wide range reflects typical ground and surface waters in the area, the $^{87}Sr/^{86}Sr$ ratios of Marcellus Shale produced waters will likely be a distinguishing characteristic compared to local shallow groundwater or surface waters, or to other high-TDS waters.

At the four sites where produced water was collected as it came out of the well, strontium (as well as other major elements not plotted) shows clear trends of increasing concentration over time (Fig. 17a). This apparently reflects progressive incorporation of salts or connate brines into the fracturing fluid. In contrast, a fairly constant ε_{Sr} of the produced waters is reached within the first two days of pumping (Fig. 17b). The one exception to this is the Greene County well, which appears to drop nearly to the value of the fracturing fluid on day 7; the reason for this anomaly is not clear. However, in most cases, individual wells produced waters with a very narrow range of ε_{Sr} values, most likely reaching a steady state value within the first few days after commencement of pumping.

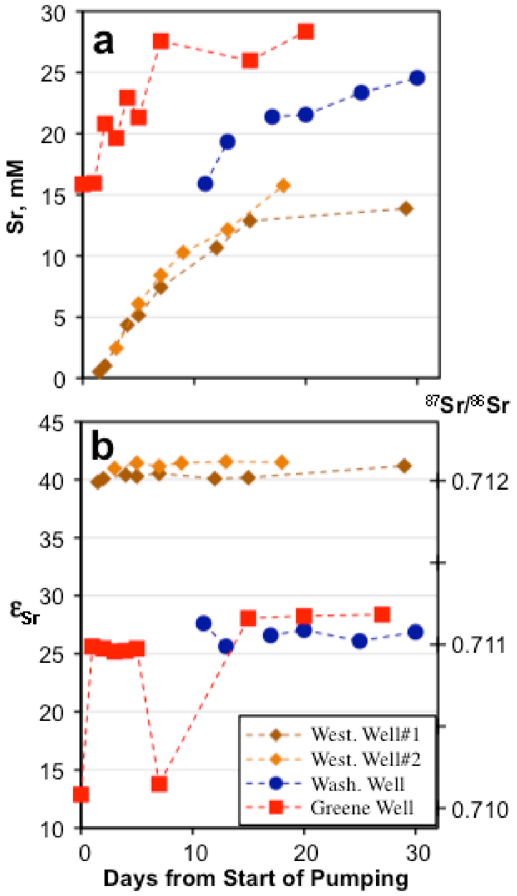

Figure 17. Variations in (a) strontium concentration and (b) ε_{Sr} (or $^{87}Sr/^{86}Sr$) plotted against the day of sample collection from the start of pumping. For the Greene County well (red squares) the point at day 0 is hydraulic fracturing fluid. In all cases, the Sr concentration starts out lower and builds gradually to near a steady state value by 30 days. In contrast, the ε_{Sr} values appear to reach a steady state value within 5-10 days after initiation of pumping, reflecting the domination of Marcellus Shale salt of brine Sr to the overall Sr budget.

3.4 DISCUSSION

3.4.1 Origin of TDS in Marcellus produced waters

The relatively narrow range of ε_{Sr} values of Marcellus Shale produced waters appears to be a distinguishing characteristic of these waters. Even when corrected for ^{87}Rb decay using available Rb concentration data, these values fall above the range of Middle Devonian seawater values, and in fact above any Phanerozoic seawater (Burke et al., 1982). If the salts or brines that are accessed by hydrofracturing are of marine origin, there must have been addition of radiogenic strontium (^{87}Sr) prior or subsequent to incorporation in the Marcellus Shale. Possible sources include the silicate portion of the shale itself (primarily clays), which should be relatively enriched in ^{87}Sr, or basinal fluids that interacted with adjacent units before being incorporated (as brine or salt) in the Marcellus Shale. Given the relative homogeneity of the Sr isotope ratios over the ~375 km distance represented by our sampling, large-scale fluid flow is a more likely source of the radiogenic Sr than localized incorporation of Sr from the shale. The somewhat bimodal distribution of values between the Westmoreland County waters and all of the others (Fig. 18) could reflect lithological variations within the Marcellus Shale section or variations in ε_{Sr} across the depositional basin. Additional produced water data combined with stratigraphic correlations will be required to characterize specific geographic trends in the Sr isotope ratios.

An important question in hydraulic fracturing is the extent to which the induced fractures remain in the target formation. If the fractures and hydrofracturing fluid come into contact with underlying or overlying formations, then additional solids could be introduced into the fluid. The Marcellus Shale in the sampling area is underlain by the Onondaga or Selinsgrive

Limestone, and is overlain by shale and limestone members of the Hamilton Group. Unaltered marine limestones would have low ε_{Sr} values (-35 to 0), whereas other shale units could be variable but are likely to be different from the Marcellus Shale. The narrow range of ε_{Sr} values from Marcellus Shale produced waters indicates significant incursions of hydrofracturing fluid into adjacent units did not occur. This is further bolstered by the apparently rapid attainment of steady state in ε_{Sr} achieved by produced waters (Fig. 17b). The drop in ε_{Sr} on day 7 of the Greene County well production could reflect incorporation of solids from another source, either within or outside of the Marcellus Shale, but this event was apparently short-lived. On the whole, the isotope variations in Marcellus produced water are best explained by interactions with salts or brines within the shale itself.

3.4.2 Signatures of Marcellus produced waters

Elevated TDS alone is not always an effective tracer of produced water contributions (Frost et al., 2010), nor are variations in concentrations of dissolved chemical species (Christian et al., 2011). Marcellus produced waters can contain high concentrations of barium, up to 12,000 mg/L (Table 5), but the concentrations can vary significantly, with low values of 10 mg/L reported here for some Washington County impoundment waters. Due to the low solubility of barite ($K_{sp}=10^{-10}$), Ba cannot be considered a conservative element in aqueous systems. The high concentrations in produced water may be stabilized by organic matter or excess Cl^-, but dilution by freshwater is likely to cause significant precipitation of barite, which may be enhanced by further oxidation of S^{2-} to SO_4^{2-} (Blount, 1977). High sodium and chloride concentrations are also characteristic of Marcellus produced waters. However, streams and rivers in populated areas often already contain significant concentrations of Na and Cl due to the use of road salt, leakage of septic systems, and wastewater outflows (Berner and Berner, 1996; Mullaney et al., 2009). In some cases, alkaline abandoned mine drainage can have Na/Ca ratios equal to or higher than those of produced water (Table 6). A modest inflow of produced water would not be easily distinguishable or quantifiable under these circumstances. Moreover, brines from abandoned and leaking oil and gas wells from shallower formations commonly contain Na, Cl, Ba, and Sr concentrations comparable to those of Marcellus produced waters (Dresel and Rose, 2010).

Similarly, carbon isotopes alone are not always sufficient in distinguishing sources of high TDS. Isotopic fingerprinting using carbon isotopes can distinguish biogenic from thermogenic methane (Kaplan et al., 1997; Laughrey and Baldassare, 1998; Révész et al., 2010; Rowe and Muehlenbachs, 1999; Schoell, 1980, 1983). However, this method cannot necessarily distinguish between different stratigraphic sources of natural gas, such as shallower natural gas sources tapped decades ago vs. a deep Marcellus Shale source, or between pipeline/storage gases and native thermogenic gas (Baldassare and Laughrey, 1997). Thermogenic methane from different units and ages can have similar methane isotopic signatures (Osborn et al., 2011a). As a result, waters related to these methane sources may not be effectively traced.

Because Marcellus produced waters have a restricted range of strontium isotope compositions, $^{87}Sr/^{86}Sr$ ratios could be a powerful tool for identifying possible sources of TDS introduced into streams or shallow aquifers. In the Appalachian region of the U.S., increases in dissolved solids to waterways can have several vectors, including road salt, drainage from inactive coal mines, leaching of coal fly ash disposal sites, and leakage of produced water from Marcellus Shale natural gas production. If the Sr concentration and isotope composition of two waters are known, then their mixing ratio can be precisely calculated, provided they have different ε_{Sr} values. The isotope ratio of the mixture is given by:

$$R_m = \frac{J_1C_1R_1 + J_2C_2R_2}{J_1C_1 + J_2C_2} \tag{1}$$

where R_m is the isotope ratio of the final mixture (expressed either as $^{87}Sr/^{86}Sr$ or ε_{Sr}), J_1 and J_2 are the fluxes of the two endmember liquids prior to mixing, C_1 and C_2 are the Sr concentrations of the endmembers, and R_1 and R_2 are the Sr isotope compositions of the endmembers. This can be rearranged to give the flux ratio:

$$\frac{J_1}{J_2} = \frac{C_2R_2 - C_2R_m}{C_1R_m - C_1R_1} \tag{2}$$

As can be seen from equation (1), the isotope ratio of the mixture will be sensitive to a component with a high Sr concentration, such as Marcellus produced waters. In a hypothetical case of produced water with 1,000 mg/L Sr and $\varepsilon_{Sr} = +25$ mixing into a stream containing 0.5 mg/L Sr with $\varepsilon_{Sr} = +50$, an addition of only 0.05% of the produced water would shift the stream ratio from +50 to +37.5, well beyond measurement precision (<±0.2).

In western Pennsylvania, drainage from abandoned coal mines (AMD) has long been a source of pollution to local waterways. In several recent cases, an increase in TDS in local waterways has been attributed both to AMD and to leakage of produced waters (PA DEP, 2009; PFBC, 2011; Renner, 2009b; Reynolds, 2009). Cases such as these can potentially be resolved using Sr isotopes to identify the source of TDS. The strontium isotope composition of AMD from a variety of localities (Table 6) tends to be higher than that of produced water, and it also varies somewhat systematically with stratigraphic position of the mined coal (Fig. 18). Though there is a limited degree of overlap in ε_{Sr} values, in most cases a clear distinction would be expected between produced water and AMD sources. The same is true of leakage from fly ash impoundments, which could have a range of ε_{Sr} values from –8 to +80 (Spivak-Birndorf et al., in press), as well as high Ba and Sr concentrations (Querol et al., 2001).

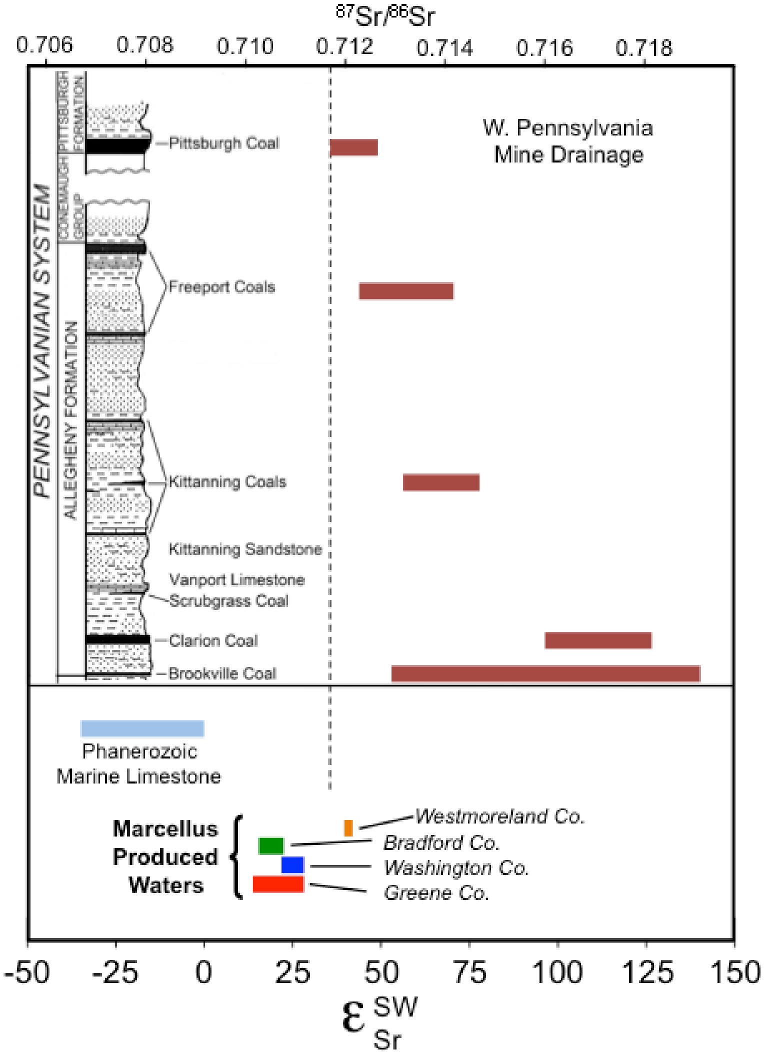

Figure 18. Strontium isotopic variations of Marcellus shale produced waters compared to western Pennsylvania AMD and Phanerozoic limestone. The Marcellus Shale produced waters define a relatively tight field compared to other possible sources of strontium in the Marcellus natural gas production region. The isotopic composition of AMD waters appears to vary systematically with stratigraphic position, with the only

overlap between AMD and produced waters coming from Pittsburgh coal AMD and produced waters from Westmoreland County. The tight clustering of Marcellus produced water values and large difference between these and other possible TDS sources indicate that Sr isotopes can be an effective tracer for produced water.

The utility of Sr isotopes in identifying and quantifying sources of TDS to waterways can be further enhanced by combining ε_{Sr} with a distinguishing chemical parameter. This study indicates that Sr/Ca ratios of produced water, while forming a basin-wide trend, tend to vary from well to well (Fig. 16a). Because both Sr and Ca are expected to be conservative tracers in these aqueous systems, combining Sr/Ca ratios with ε_{Sr} values is likely to distinguish between sources in nearly all cases. To demonstrate, mixing equations were calculated for a hypothetical stream with an isotope ratio (ε_{Sr} = +35) between those of the Westmoreland County produced waters and all other produced waters, but with Sr/Ca ratios typical of natural streams. Mixing curves were generated for this stream interacting with Marcellus produced waters, acid mine drainage from the Pittsburgh coal seam, and brines drawn from abandoned oil wells tapping the Venango formation (Fig. 19; Chapman et al., in prep). Produced waters from each well or region fall in a unique region of Sr/Ca-ε_{Sr} space. Using the mean values as mixing endmembers, the shift in Sr/Ca and ε_{Sr} resulting from addition of the produced waters or AMD to a stream can be calculated; the labeled tick marks on the curves indicate the percentage of produced water or AMD required to generate the observed shift. In some cases, a flux equivalent to only 0.01% of the stream flow results in significant shifts of the stream water isotope ratios, and a 0.1% addition moves the Sr/Ca and ε_{Sr} of the stream up to halfway toward the produced water endmember values. In all cases, the stream ε_{Sr} value is completely dominated by produced water when the produced water flux reaches 1% of the stream flow. In contrast, more AMD (>10%) would be required to shift stream waters significantly toward AMD ε_{Sr} values. Because the AMD inflows in any given location are likely to be significantly different in ε_{Sr} from Marcellus produced waters, this method is likely to yield definitive evidence for the source of TDS contamination. In the event of a produced water spill, the amount of produced water or other contaminant entering the stream can be quantified. It should be noted that the example shown in Figure 19 is for a stream with an isotopic composition similar to Marcellus produced waters. Streams with ε_{Sr} values greater than about +50, which are likely to be common in the Appalachian Basin, will be even more sensitive to influxes of Marcellus produced waters.

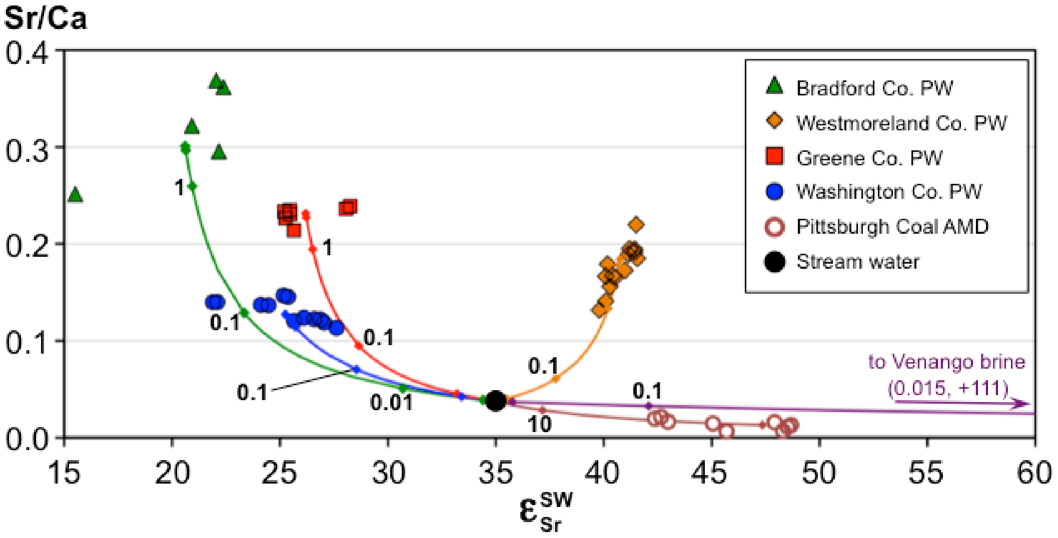

Figure 19. Mixing curves for a hypothetical stream being impacted by Marcellus produced waters, acid mine drainage, and Venango Fm. oil well brines. The produced waters are separated in Sr/Ca-ε_{Sr} space by geographic location. For each endmember, a weighted mean value is used to calculate the mixing curve, and individual samples are shown for comparison (except for Venango brines, which plot off scale). The labeled tick marks on the curve indicate the percent flux of each endmember added to the hypothetical stream water. Only a very small amount of produced water (0.01-0.1%) added to the stream can produce large shifts in ε_{Sr} of 5-15 ε units (note that typical measurement uncertainty is <0.02 ε units). Just a 1% addition of produced water will shift the stream isotopic composition completely to the ε_{Sr} of the produced water. Much larger amounts of AMD are required to shift the isotopic composition of the stream toward that endmember.

3.5 CONCLUSIONS

An approach that integrates geochemistry, hydrogeology, and knowledge of historic energy extraction activities is critical to the successful remediation of existing water quality problems and the protection of water resources in the Appalachian Basin and other geologically and hydrochemically complex areas. These data suggest that the Sr isotope ratios constitute an extremely sensitive tracer with strong potential as a tool for verification of safe water disposal, and can be used to determine the origin of TDS in surface and ground waters affected by multiple sources as well as to quantify mixing between them.

4.0 FORM AND ORIGIN OF SALTS IN THE MARCELLUS SHALE AND ADJACENT UNITS: GEOCHEMICAL AND STRONTIUM ISOTOPIC ANALYSIS OF SEQUENTIAL EXTRACTIONS

4.1 INTRODUCTION

The economical extraction of natural gas from low-permeability reservoirs using the combined technologies of horizontal drilling and hydraulic fracturing has greatly increased within the past few decades. Black shale gas plays in particular have seen rapid growth since the 1950s, with this growth continuing through the development of the Marcellus Shale play within the last five years (U.S. EIA, 2011b). Concurrent with natural gas production, hydraulic fracturing has resulted in large volumes of produced waters with extremely high levels of dissolved solids (TDS), leading to questions about the origin of these solids in the Marcellus Shale itself.

The Marcellus Shale forms the base of the Middle Devonian Hamilton Group, and is the deepest of a series of eastward-thickening black shales. It is a black, organic-rich shale that formed under anoxic conditions in a restricted basin following the Acadian orogeny (Kargbo et al., 2010; Lash, 2008; Lash and Engelder, 2009). The Marcellus Shale consists of two intervals of black shale (the Oatka Creek and Union Springs Members) separated by an interval of limestone (the Cherry Valley Limestone; Lash and Engelder, 2011). The base of the Marcellus Shale is more than 2,700 m deep along its southeastern margin (Lash and Engelder, 2011).

Because the shale functions as both source rock and reservoir rock for natural gas, it is considered an unconventional reservoir, requiring both horizontal drilling and hydraulic fracturing for economic recovery of gas.

Hydraulic fracturing of a typical Marcellus Shale well requires 8-15 million liters of water (Kerr, 2010). A portion of this water is returned from the well, along with possible formation brines. These produced waters acquire high concentrations of total dissolved solids (often exceeding 150,000 mg/L; Chapman et al., in review), but the source of the dissolved solids in Marcellus Shale produced water is unclear. Many formation brines are inferred to have a significant evaporated seawater component (Rowan and De Marsily, 2001; Stueber and Walter, 1991); however, significant amounts of water have not been reported when drilling into the Marcellus Shale. Conversely, Blauch et al. (2009) found lenticular salt deposits in a Marcellus Shale core sample, and hypothesized that the high salinity is from autochthonous salts. Understanding the source of these salts and metals can be useful in designing exploration and drilling strategies. For example, drillers could avoid high-salinity areas in the shale, thus minimizing the amount of treatment required for produced waters. Additionally, knowledge of the form and origin of the salts can help to clarify heterogeneities in properties such as organic matter and productivity.

To understand the form and reservoirs of major salts and metals in the Marcellus Shale, a four-step chemical sequential extraction procedure was performed on dry-drilled well cuttings from a well in Tioga County, NY. In this study, major, minor, and trace elements as well as strontium isotopes are reported for nine samples. Geochemical and isotopic analysis was applied to identify reservoirs where salts are held in the shale, and to understand compositional differences between the upper and lower members.

Strontium isotopes have been used to track formation brine evolution, as well as to understand post-depositional processes in shale and salt deposits (Armstrong et al., 1998; Barnaby et al., 2004; Carlson, 1987; McNutt et al., 1987; Perry Jr and Turekian, 1974; Stueber et al., 1993). Additionally, the Sr isotopic composition of the extractions can be compared to the values measured for Marcellus Shale produced waters (Chapman et al., in review) to understand the source of dissolved solids in those waters. Similarly, information on the evolution and post-depositional changes of the shale can be gained by comparing the Sr isotope values of the leachates to that of Middle Devonian seawater.

4.2 MATERIALS AND METHODS

4.2.1 Samples

Samples were obtained as dry-drilled well cuttings (grain size <1 mm) from a well drilled in Tioga County, NY, in November 2009 (Figure 20). Each sample was collected as a composite sample, which contained 3-9 m of drilled material; for units above the Marcellus Shale, the sampling interval was 9 m, and for the Marcellus Shale and lower units, the sampling interval was 3 m. Sequential extraction and XRD analysis were performed on a subset of nine samples with median sampling depths ranging from 901 to 1,434 m (Fig. 21; Johnson and Graney, 2011). Based on a wireline log from a nearby (<5 km away) well, the proposed units from which the samples came are Tully Limestone (one sample); Undifferentiated Hamilton (two samples); Marcellus Shale (four samples); Onondaga Limestone (one sample); and Oriskany Sandstone (one sample). The Marcellus Shale samples were readily identifiable as dark, black powders, compared to the gray color of the rest of the samples. According to personal communication with the drillers, the unit directly below the Marcellus, proposed to be the Onondaga Limestone, was markedly harder than surrounding units. Additionally, none of the units encountered during drilling (below freshwater aquifers) contained significant amounts of formation waters; the Marcellus Shale samples came up slightly damp, and were air-dried before being placed in sample vials. All samples effervesced in 8% acetic acid (see sequential extraction method, below), indicating that some carbonate was present.

Figure 20. Photograph of drill cuttings as received. The gray sample is from the Hamilton Group, and the black sample is Marcellus Shale. Photograph taken by Jason Johnson of Binghamton University.

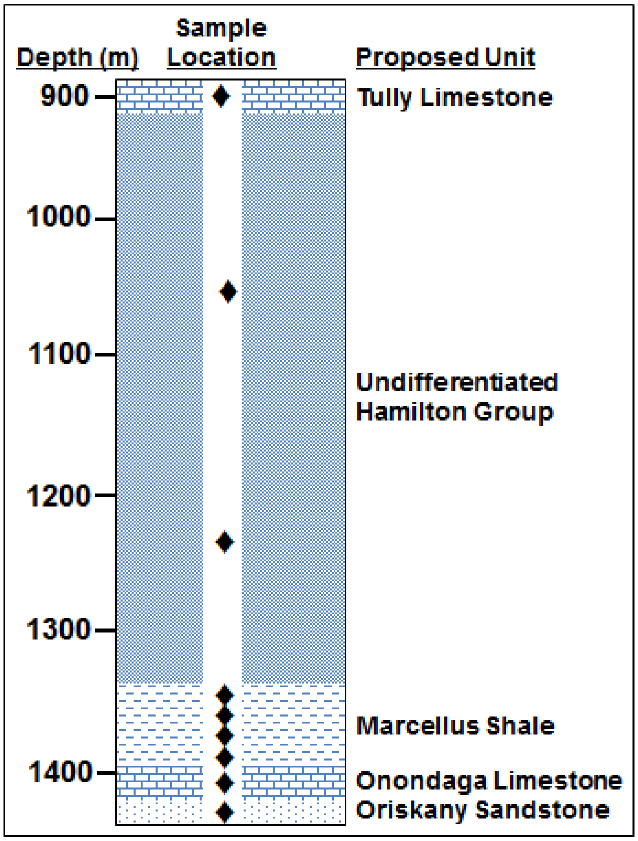

Figure 21. Generalized stratigraphic section of Devonian-age units neighboring the Marcellus Shale. the Marcellus forms the base of the Hamilton Group. The depths of the nine core samples are designated by black diamonds. Modified from Johnson and Graney, 2011.

4.2.2 Sequential extraction method

A four-step chemical sequential extraction procedure (Fig. 22) was performed on the samples as received; the grain size for all samples was <1 mm. The procedure was designed to target different soluble element reservoirs and mineral phases in the samples. First, ~0.5 g splits of crushed material were added to acid-washed, preweighed 50 mL centrifuge tubes. The tubes were reweighed, and then ~30 mL of ultrapure water was added. This leach targeted water-soluble salts and sulfates. Samples were shaken for 24 h, centrifuged, and the leachant was pipetted and filtered to <0.45µm into preweighed, acid-washed 60 mL polypropylene bottles.

Then, ~20 mL of ultrapure water was added to the tubes, which were briefly shaken, centrifuged, and pipetted and filtered into the same 60 mL bottles. After these bottles were reweighed, a 3 mL aliquot was taken to measure pH, and another 3 mL aliquot was taken for anion analysis, after which the 60 mL bottles were reweighed. Then, 1 mL concentrated ultrapure nitric acid was added to the 60 mL bottles to acidify the samples for major and trace cation analysis.

Next, ~30 mL 1N ultrapure ammonium acetate buffered to pH 8 was added to the tubes, which were shaken overnight, centrifuged, pipetted and filtered into acid-washed polymethylpentene (PMP) beakers. An additional ~20 mL ammonium acetate was added, centrifuged, pipetted and filtered into the PMP beakers, then dried at 100°C. This leach targeted exchangeable cations bound to clays. Next, ~30 mL 8% ultrapure acetic acid was added to the tubes, and the same process was repeated to target carbonate minerals. After the acetic acid leach, ~30 mL 0.1N ultrapure hydrochloric acid was added and the process was repeated. This leach targeted other acid-soluble phases.

After the ammonium acetate, acetic acid, and hydrochloric acid leaches were completely dried, they were transferred using 2% ultrapure nitric acid into acid-washed, preweighed 60 mL polypropylene bottles which were then reweighed. The residue left in the centrifuge tubes was transferred using ultrapure water into acid-washed, preweighed PMP beakers, dried at 100°C, and reweighed.

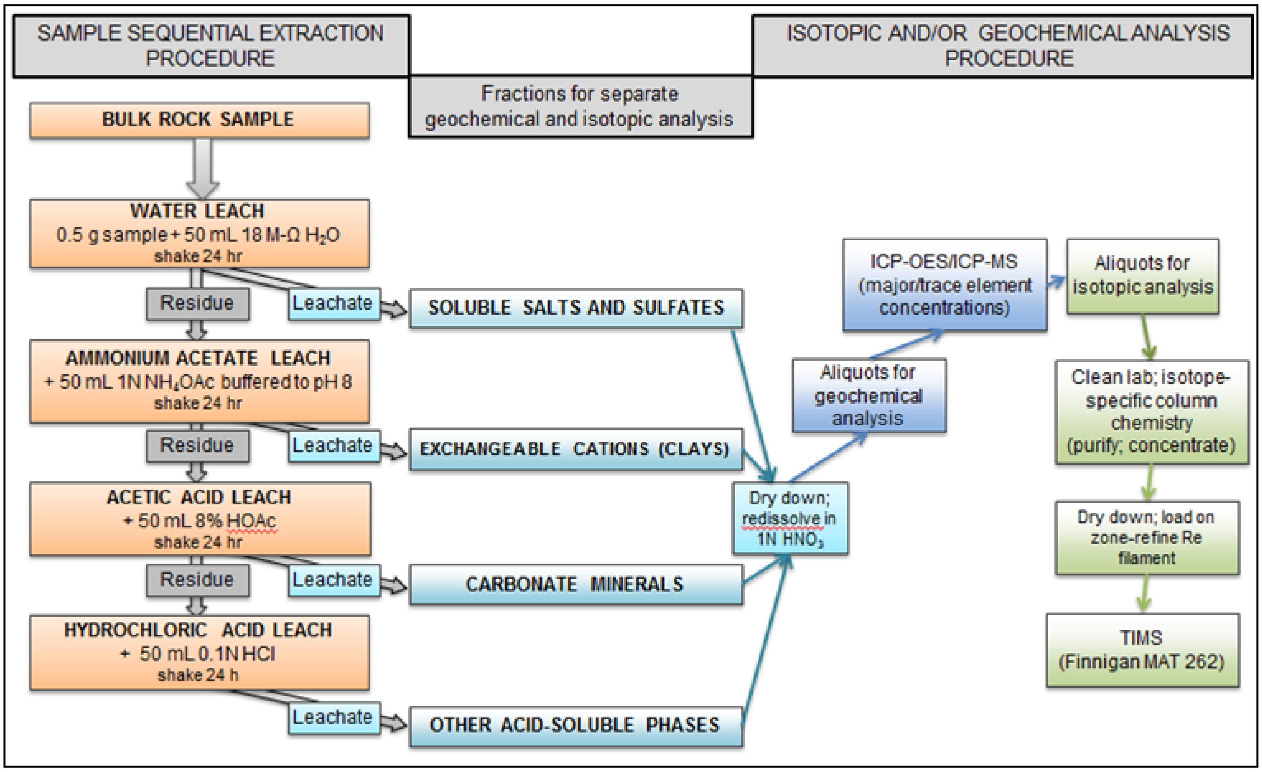

Figure 22. Flowchart describing sequential extraction procedure.

4.2.3 Analytical methods

X-ray diffraction (XRD) analyses were performed by Jason Johnson of Binghamton University. To prepare the drill cuttings for analysis, a mortar and pestle was used to mill the samples to a fine powder. XRD analysis was performed on a PANalytical X'Pert PRO MPD X-ray diffractometer with Cu Kα radiation at Bucknell University. Peak positions (d-spacings) were determined using the IdeCom software program.

Leachates were analyzed for major and trace cations by ICP-MS and ICP-OES at DOE-NETL Pittsburgh. The water leachates were also analyzed for major anions by ion chromatography, also at DOE-NETL Pittsburgh.

Preparation for Sr isotope analysis was carried out under clean lab conditions at University of Pittsburgh. Aliquots containing between 0.8 and 5 µg Sr, as determined by ICP-OES, were evaporated to dryness and redissolved in 6N ultrapure nitric acid. Samples were then eluted through columns containing Eichrom® Sr resin in order to separate Sr from all other constituents in the sample. Column eluents were collected in acid-washed Teflon vials, evaporated to dryness, and redissolved in 2N ultrapure nitric acid. For each sample, an aliquot containing ~500 ng Sr was evaporated onto a rhenium filament pre-loaded with a tantalum oxide carrier agent. To measure Sr isotopes of the samples as well as the Sr standard SRM 987, a multidynamic method on a Finnigan MAT 262 thermal ionization mass spectrometer was used. The average $^{87}Sr/^{86}Sr$ ratio of SRM 987 over the period of these analyses was 0.710244, with an estimated external reproducibility of ±0.000015.

Strontium isotope ratios are presented using ε_{Sr}^{SW} (or ε_{Sr}) notation, where the $^{87}Sr/^{86}Sr$ ratio of the sample is normalized to the globally uniform $^{87}Sr/^{86}Sr$ ratio of present-day seawater:

$$\varepsilon_{Sr}^{SW} = 10^{4}\left(\frac{^{87}Sr/^{86}Sr_{sample}}{^{87}Sr/^{86}Sr_{seawater}} - 1 \right)$$

Our measured seawater $^{87}Sr/^{86}Sr$ value is 0.709170.

4.3 RESULTS

4.3.1 Mineralogy

Table 7 shows the portion of each sample that dissolved after all four sequential extractions. The greatest amount of dissolution (60%) occurred in sample 6, proposed to be from the Tully Limestone. Samples 82 (Oriskany Sandstone?) and 78 (Onondaga Limestone?) also showed significant amounts of dissolution (49 and 31%, respectively). The low percentage of sample dissolution in these limestone samples indicates that these are not 'clean' limestones, but rather contain significant amounts of silicate material that was not dissolved by acetic acid.

Only 8% dissolution occurred in samples 22 and 41, proposed to be undifferentiated Hamilton Group material. The four Marcellus Shale samples (54, 61, 65, and 71) showed marked differences in % dissolved between the two upper and two lower samples. The two upper Marcellus Shale samples had the least amount of dissolution out of all samples (6 and 3%), whereas the two lower samples both showed much higher amounts of dissolution (14 and 26%), indicating that the lower member of the shale contains a greater amount of carbonate minerals than the upper one. This is supported by the identification of calcite, which may be present as carbonate cements or lenses, in samples 65 and 71 by XRD (Fig. 23).

Table 7. Percent sample dissolved after four-step (water - ammonium acetate - acetic acid - HCl) sequential extraction, compared to mineralogical data from Johnson and Graney, 2011, and personal communication

Sample	Proposed Unit	Median Depth m	% Sample Dissolved[a]	Quartz	Calcite	Pyrite	Muscovite/ Illite[b]	Chlorite group
6	Tully Ls.?	901	60%	x[c]	XX	-	X	X
22	Hamilton Gp.	1046	8%	X	-	-	X	X
41	Hamilton Gp.	1221	8%	X	-	-	X	X
54	Marcellus Sh.	1337	6%	X	-	X	X	X
61	Marcellus Sh.	1358	3%	X	-	X	X	X
65	Marcellus Sh.	1370	14%	X	X	XX	X	-
71	Marcellus Sh.	1389	26%	X	XX	X	X	-
78	Onondaga Ls.?	1410	31%	X	X	-	X	-
82	Oriskany Ss.?	1434	49%	XX	XX	-	X	-

[a] Total % of residue dissolved after all four sequential extractions

[b] Similar major peaks make muscovite and illite difficult to distinguish

[c] Lowercase x: low signal intensity; capital X: high intensity; double uppercase XX: highest intensity; dash: none detected

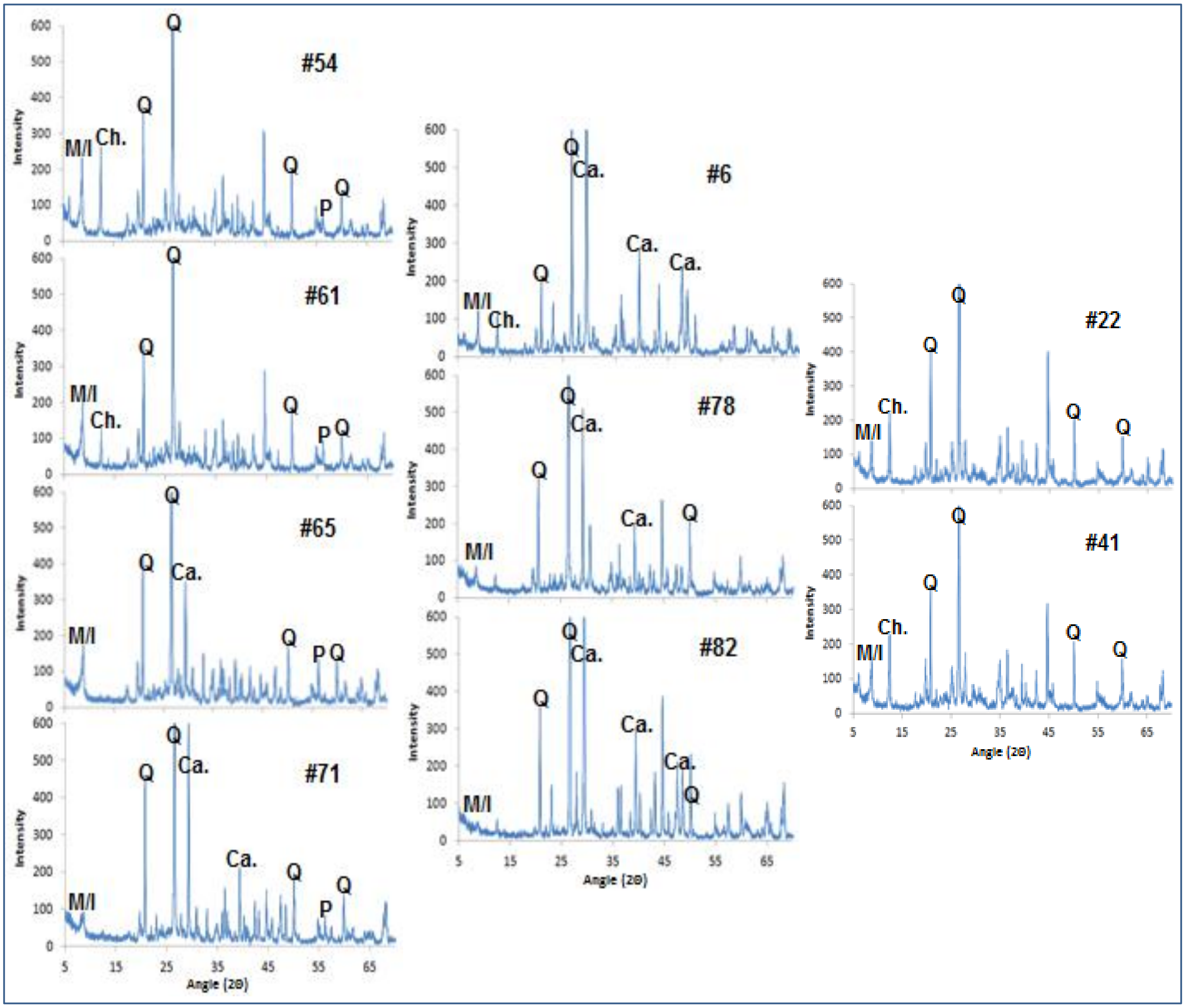

Figure 23. XRD patterns for the nine drill cutting samples. Marcellus Shale samples are in the left column; the center column shows the limestone and sandstone samples; Hamilton Group samples are in the right column. Q = quartz; Ca. = calcite; P = pyrite; M/I = muscovite/illite; Ch. = chlorite. Analysis was performed at Bucknell University by Jason Johnson of Binghamton University.

Sample 6, proposed to be from the Tully Limestone unit, contains minor amounts of quartz and greater amounts of muscovite/illite, and chlorite. The primary mineral phase in this sample is calcite. Samples 22 and 41, proposed to be undifferentiated Hamilton Group material, contain quartz, muscovite/illite, and chlorite minerals. The four samples of Marcellus Shale have varying amounts of calcite, with the two deeper samples (65 and 71) having more than the two upper ones (54 and 61). Conversely, the upper two samples contain chlorite, whereas the lower two do not. All Marcellus Shale samples contain muscovite/illite and pyrite, with sample 65 exhibiting a greater intensity in pyrite peaks.

Sample 78, assigned as Onondaga Limestone, contains quartz, calcite, and muscovite/illite; even though it is proposed to be a limestone, calcite did not appear to be the dominant mineral. In New York, the Onondaga comprises carbonate platform facies, with calcarenitic to cherty to argillaceous limestones and minor shales (Brett and Baird, 1996), suggesting that it could contain significant amounts of quartz. Sample 82, proposed to be the Oriskany Sandstone, exhibited strong peak intensities for quartz and calcite, with significant amounts of muscovite/illite as well. Basan et al. (1980) described Oriskany lithologies ranging from quartz arenites to calcareous sandstones and sandy limestones in the Appalachian Basin, suggesting that significant amounts of carbonate could be present in this unit. Based on their lithologic similarities, these units may be difficult to discern based on drill cutting samples alone.

4.3.2 Geochemistry

Geochemical data of the leached materials are presented in Table 8. Over 80% of the total Br and Na leached was released in the water extraction. While Cl was only measured in the water leach, a relatively large amount (356 to 1,912 µg/g) was extracted by water. The ammonium acetate extraction liberated significant portions of the leached Ba (58-79%). The majority of Ca, Fe, Mg, and Mn that were leached dissolved in the acetic acid extraction. The greatest portion of Al leached (>57%) was extracted by HCl. Leachable Sr was variable between the four extractions. In samples with greater amounts of leached Ca, and greater intensities of calcite (as determined by XRD; samples 6, 65, 71, 78, and 82), the majority of the Sr leached was released in the acetic acid extraction. For the rest of the samples (22, 41, 54, and 61), the majority of Sr leached was extracted by water or ammonium acetate.

Table 8. Major and trace element composition of sequentially extracted drill cuttings

Sample	Proposed Unit	Leaching Solution	Targeted Phase	Al	Ba	Br	Ca	Fe	K	Mg	Mn	Na	Rb	S	Si	Sr	Cl
				μg leached/g sample													
6	Tully Ls.?	water	salts, sulfates	85	22	3.87	632	25	153	45	0.456	346	0.35	75	174	12	356
22	Hamilton Gp.	water	salts, sulfates	219	25	NA[d]	584	355	215	109	3.32	846	1.8	29	265	35	1,193
41	Hamilton Gp.	water	salts, sulfates	213	31	NA	420	346	214	96	3.28	919	3.2	35	263	27	979
54	Marcellus Sh.	water	salts, sulfates	102	45	7.6	369	184	140	72	1.88	647	0.78	304	131	19	662
61	Marcellus Sh.	water	salts, sulfates	9.6	33	8.8	700	25	80	87	1.06	780	0.41	410	29	24	665
65	Marcellus Sh.	water	salts, sulfates	34	24	11	848	45	119	53	0.323	727	0.45	494	74	41	780
71	Marcellus Sh.	water	salts, sulfates	48	29	16	886	79	78	48	0.721	837	0.23	287	107	49	1,231
78	Onondaga Ls.?	water	salts, sulfates	87	44	22	875	115	283	147	0.835	862	0.95	72	154	92	1,912
82	Oriskany Ss.?	water	salts, sulfates	37	8.4	3.98	741	44	121	58	0.302	231	0.44	81	89	15	386
6	Tully Ls.?	amm. ac.[a]	exchangeables	<0.01	357	0.718	11,923	14	52	200	27	19	0.75	299	42	28	NA
22	Hamilton Gp.	amm. ac.	exchangeables	8.1	113	0.832	4,356	33	75	224	70	21	1.0	71	33	40	NA
41	Hamilton Gp.	amm. ac.	exchangeables	14	193	3.76	5,601	31	113	317	85	27	1.6	93	56	61	NA
54	Marcellus Sh.	amm. ac.	exchangeables	7.3	628	0.661	1,462	24	99	295	23	22	1.4	196	28	43	NA
61	Marcellus Sh.	amm. ac.	exchangeables	3.6	798	<0.05	2,254	12	123	388	11	27	2.1	414	29	39	NA
65	Marcellus Sh.	amm. ac.	exchangeables	<0.01	208	1.99	8,839	9	120	170	13	33	1.8	373	25	59	NA
71	Marcellus Sh.	amm. ac.	exchangeables	<0.01	152	2.95	8,951	20	55	98	7.6	23	0.75	291	27	47	NA
78	Onondaga Ls.?	amm. ac.	exchangeables	<0.01	200	0.552	13,058	16	110	312	17	27	1.4	235	36	87	NA
82	Oriskany Ss.?	amm. ac.	exchangeables	<0.01	59	0.450	14,416	17	39	124	9.7	15	0.43	242	39	26	NA
6	Tully Ls.?	acetic[b]	carbonates	216	31	<0.05	182,662	4,876	28	4,669	689	101	0.13	2,712	187	261	NA
22	Hamilton Gp.	acetic	carbonates	235	5.2	0.305	4,282	2,036	23	1,055	243	7.5	0.27	25	182	6.9	NA
41	Hamilton Gp.	acetic	carbonates	250	8.4	0.309	6,414	3,168	27	1,578	328	9.5	0.34	62	193	10	NA
54	Marcellus Sh.	acetic	carbonates	136	50	0.153	4,225	2,834	14	1,331	111	5.8	0.20	63	117	6.7	NA
61	Marcellus Sh.	acetic	carbonates	84	95	0.169	3,968	2,507	7	1,166	38	4.7	0.14	75	74	7.7	NA
65	Marcellus Sh.	acetic	carbonates	72	15	0.308	26,801	2,836	11	1,940	80	23	0.15	383	68	71	NA
71	Marcellus Sh.	acetic	carbonates	46	15	0.449	69,847	683	6	3,575	75	47	0.07	870	61	136	NA
78	Onondaga Ls.?	acetic	carbonates	180	18	0.463	54,644	4,929	27	4,977	131	56	0.34	895	149	114	NA
82	Oriskany Ss.?	acetic	carbonates	113	6.2	<0.05	145,358	2,993	17	2,186	105	60	0.09	1,718	111	154	NA
6	Tully Ls.?	hydrochloric[c]	other acid-soluble phases	441	206	0.262	1,881	1,219	102	492	18	11	1.2	26	58	3.9	NA
22	Hamilton Gp.	hydrochloric	other acid-soluble phases	1147	5.8	0.603	779	2,833	118	416	20	16	1.9	<0.03	156	3.5	NA
41	Hamilton Gp.	hydrochloric	other acid-soluble phases	1091	12	0.554	942	2,742	159	511	24	19	2.2	4	143	3.5	NA
54	Marcellus Sh.	hydrochloric	other acid-soluble phases	591	186	0.370	705	2,121	78	273	11	13	1.4	182	76	6.1	NA
61	Marcellus Sh.	hydrochloric	other acid-soluble phases	246	178	0.486	1,024	1,849	78	290	9.6	15	1.2	355	41	6.5	NA
65	Marcellus Sh.	hydrochloric	other acid-soluble phases	142	37	0.482	2,395	1,428	73	637	14	16	1.2	451	57	9.4	NA
71	Marcellus Sh.	hydrochloric	other acid-soluble phases	174	42	0.604	4,924	1,570	40	2,073	17	15	0.74	296	87	13	NA

Table 8 cont.

78	Onondaga Ls.?	hydrochloric	other acid-soluble phases	308	17	0.822	14,118	3,296	165	6,175	43	22	1.7	245	70	14	NA
82	Oriskany Ss.?	hydrochloric	other acid-soluble phases	339	3.5	0.353	1,750	1,542	64	212	9.7	14	0.7	13	34	5.5	NA

[a] Ammonium acetate

[b] Acetic acid

[c] Hydrochloric acid

[d] NA = not analyzed

4.3.3 Strontium isotope composition

Strontium isotope compositions for the leachates are presented in Table 9 and Figure 24. All samples exhibit decreasing ε_{Sr} values through the first three extractions, followed by an increase in ε_{Sr} in the HCl extraction. ε_{Sr} values for the water leach range from +6.0 to +28.4, with a general decrease with depth. The water-soluble portion of the Marcellus Shale samples have ε_{Sr} values between +13.5 and +24.0, all of which fall within the range previously reported for Marcellus produced waters (Chapman et al., in review). Additionally, the ammonium acetate extractions of Marcellus Shale samples have ε_{Sr} values which fall within this range or just below it (+3.0 to +19.5). Through all four extractions, the ε_{Sr} values of Marcellus Shale samples decrease with depth. The acetic acid leachates of the two lower Marcellus Shale samples and sample #6 (Tully Ls.) have ε_{Sr} values that approach or reach the range for Middle Devonian seawater (-19.3 to -13.7; Fig. 24). The ε_{Sr} values of the HCl extractions are, for most samples, the highest out of the four leachates, indicating that HCl is accessing a source of more radiogenic (higher $^{87}Sr/^{86}Sr$) strontium.

Table 9. Strontium isotope data for sequentially extracted drill cuttings

Sample	Proposed Unit	Leaching Solution	$^{87}\mathrm{Sr}/^{86}\mathrm{Sr}$[d]			ε_{Sr}		
6	Tully Ls.?	water	0.710854	±	11	23.74	±	0.16
22	Hamilton Gp.	water	0.711183	±	10	28.39	±	0.14
41	Hamilton Gp.	water	0.711104	±	09	27.27	±	0.13
54	Marcellus Sh.	water	0.710869	±	12	23.96	±	0.17
61	Marcellus Sh.	water	0.710414	±	11	17.54	±	0.16
65	Marcellus Sh.	water	0.710131	±	10	13.54	±	0.14
71	Marcellus Sh.	water	0.710128	±	10	13.51	±	0.14
78	Onondaga Ls.?	water	0.709596	±	09	6.01	±	0.13
82	Oriskany Ss.?	water	0.710010	±	08	11.84	±	0.11
6	Tully Ls.?	amm. ac.[a]	0.709870	±	11	9.87	±	0.16
22	Hamilton Gp.	amm. ac.	0.710454	±	11	18.11	±	0.16
41	Hamilton Gp.	amm. ac.	0.710451	±	11	18.07	±	0.16
54	Marcellus Sh.	amm. ac.	0.710553	±	10	19.50	±	0.14
61	Marcellus Sh.	amm. ac.	0.710134	±	10	13.59	±	0.14
65	Marcellus Sh.	amm. ac.	0.709398	±	11	3.22	±	0.16
71	Marcellus Sh.	amm. ac.	0.709382	±	09	2.99	±	0.13
78	Onondaga Ls.?	amm. ac.	0.709304	±	11	1.89	±	0.16
82	Oriskany Ss.?	amm. ac.	0.709420	±	09	3.53	±	0.13
6	Tully Ls.?	acetic[b]	0.708189	±	14	-13.83	±	0.20
22	Hamilton Gp.	acetic	0.709451	±	11	3.96	±	0.16
41	Hamilton Gp.	acetic	0.709330	±	12	2.26	±	0.17
54	Marcellus Sh.	acetic	0.709773	±	09	8.50	±	0.13
61	Marcellus Sh.	acetic	0.709257	±	10	1.23	±	0.14
65	Marcellus Sh.	acetic	0.708278	±	08	-12.58	±	0.11
71	Marcellus Sh.	acetic	0.708250	±	10	-12.97	±	0.14
78	Onondaga Ls.?	acetic	0.708585	±	12	-8.25	±	0.17
82	Oriskany Ss.?	acetic	0.708768	±	10	-5.67	±	0.14
6	Tully Ls.?	hydrochloric[c]	NA[f]			NA		
22	Hamilton Gp.	hydrochloric	NA			NA		
41	Hamilton Gp.	hydrochloric	NA			NA		
54	Marcellus Sh.	hydrochloric	0.711276	±	08	29.70	±	0.11
61	Marcellus Sh.	hydrochloric	0.710516	±	10	18.98	±	0.14
65	Marcellus Sh.	hydrochloric	0.709835	±	07	9.38	±	0.10

Table 9 cont.

71	Marcellus Sh.	hydrochloric	0.708917	±	09	-3.57	±	0.13
78	Onondaga Ls.?	hydrochloric	0.710423	±	10	17.67	±	0.14
82	Oriskany Ss.?	hydrochloric	NA			NA		

[a] Ammonium acetate

[b] Acetic acid

[c] Hydrochloric acid

[d] Uncertainty in last two decimal places of $^{87}Sr/^{86}Sr$ ratio.

[e] $\varepsilon_{Sr} = (^{87}Sr/^{86}Sr_{sample}/^{87}Sr/^{86}Sr_{seawater} - 1)\bullet 10^4$; measured $^{87}Sr/^{86}Sr_{seawater} = 0.709170$.

[f] NA = not analyzed

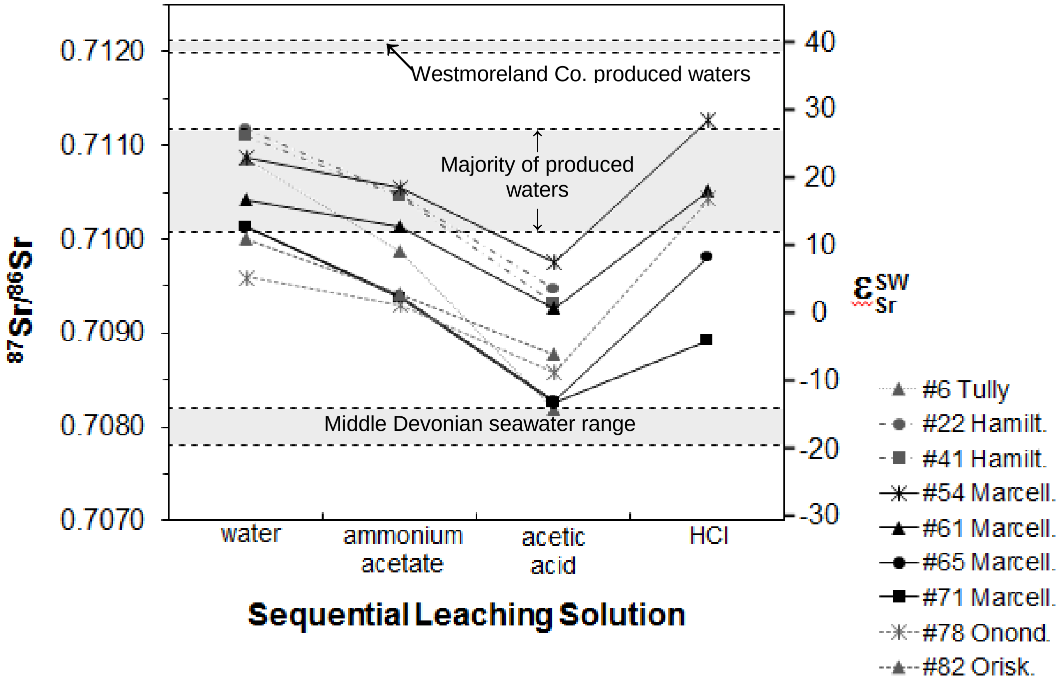

Figure 24. Sr isotopic composition of sequential extractions compared to ranges for Marcellus produced water and Middle Devonian seawater.

4.4 DISCUSSION

4.4.1 Primary reservoirs of Na, Ba, Ca, and Sr

Because the Marcellus Shale is the unit of interest in this study, geochemical discussion will focus on leachates from samples #54, 61, 65, and 71. Figure 25 summarizes the amounts of Na, Ba, Ca, and Sr extracted per leachant for the four Marcellus samples. Plots in the left column show the data as µg leached/g sample; plots in the right column show the data as % of total leached.

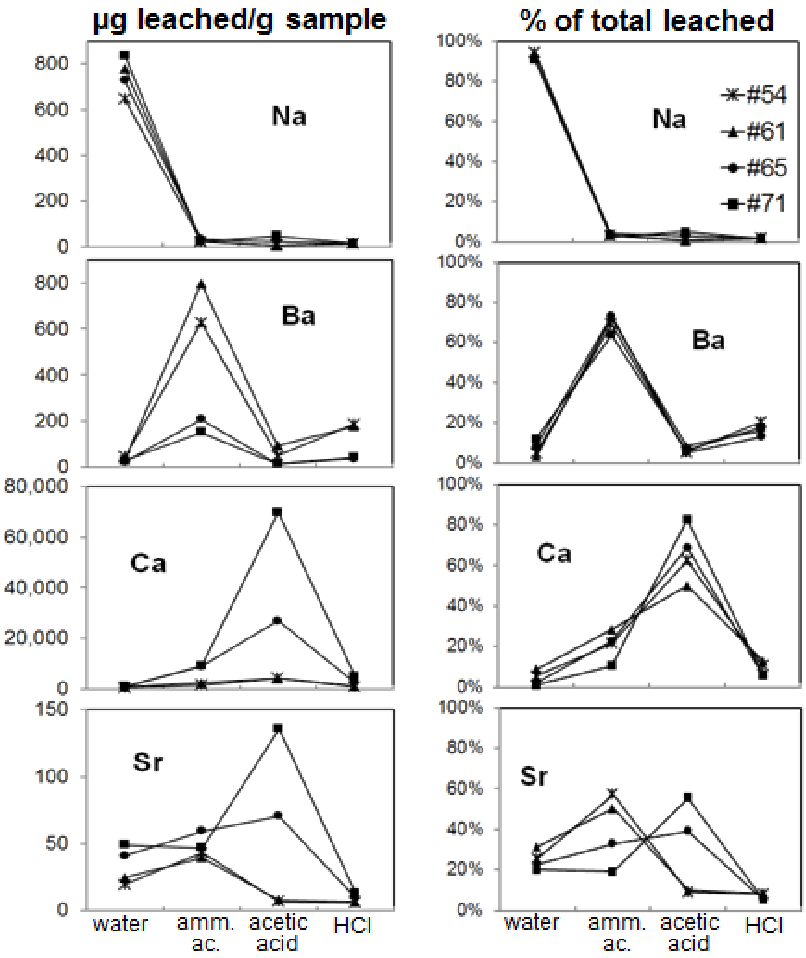

Figure 25. Na, Ba, Ca, and Sr sequentially leached from Marcellus Shale samples. Y-axis units for plots in the left column are µg leached/g sample; y-axis units for plots in the right column are % of total leached. Amm ac. = ammonium acetate.

Greater than 90% of the total Na leached was extracted by water, indicating that Na is held in soluble salts within the shale. A similar trend is seen for Br (not shown), indicating that it is also held as a soluble salt. As Marcellus Shale produced water typically contains high amounts of Na and Br (Keister, 2010; Yoxtheimer, 2011), it is not surprising that these elements are readily extractable.

The trend seen for Ba, however, was less expected. Less than 20% of the total Ba leached was extracted by water; the majority (58-79%) was extracted by ammonium acetate. This indicates that Ba is not readily extracted by water alone, but rather is held either as an exchangeable ion on clay surfaces, or as barite ($BaSO_4$), which has low solubility in water ($K_{sp}=10^{-10}$; Blount, 1977) but greater solubility in high-ionic strength solutions (Risthaus et al., 2001). The high (>2000 mg/L) concentrations of Ba characteristic of Marcellus produced water (Chapman et al., in review; Keister, 2010; Yoxtheimer, 2011) may be a reflection of the high-ionic strength solution, either hydraulic fracturing fluid or formation brines, present in the Marcellus Shale during drilling and fracturing, coupled with significant reservoirs of Ba.

Most (43-93%) of the leached Ca was extracted by acetic acid, indicating that Ca is held in a carbonate phase. Furthermore, the leached portions of the two lower Marcellus samples (#65 and 71) had 6 to 15x higher concentrations of Ca than the leached portions of the upper Marcellus samples (#54 and 61), which suggests that the lower samples contain more carbonate. Also in the lower samples, the majority of Sr leached was extracted by acetic acid, indicating that Sr is also held in the carbonate phase of these samples. Conversely, most of the Sr leached from the upper Marcellus samples was extracted by ammonium acetate; this suggests that it is held as an exchangeable ion on clay surfaces. This relationship between Sr extraction and carbonate content was observed in the non-Marcellus samples as well.

4.4.2 Evidence for post-depositional fluid flow

The Sr isotopic composition of the Marcellus Shale leachates is compared to the ε_{Sr} ranges measured for Marcellus produced waters and Middle Devonian seawater in Figure 24. The water leachates have ε_{Sr} values that fall within the range of produced waters, indicating that the dissolved solids in the produced waters originate within the Marcellus Shale itself. The ammonium acetate leachates, whose ε_{Sr} values fall within or just below the values for produced waters, also indicate that the dissolved solids originate within the Marcellus; however, the ammonium acetate may also be leaching some less radiogenic Sr that is attached to clay surfaces. The ammonium acetate was buffered to a pH of 8, so it is unlikely that there was significant carbonate dissolution, which would have contributed Sr with even lower ε_{Sr} values.

The acetic acid leachates of the Marcellus samples do not reach the ε_{Sr} values for Middle Devonian seawater, even when corrected for ^{87}Rb decay. Therefore, the Sr held in carbonate minerals within the shale does not reflect seawater Sr at the time of deposition, but rather implies some later exchange process, such as clastic sediment input or basin-wide fluid flow, either during burial or post-deposition. Due to the uniform Sr isotopic composition of Marcellus produced waters over a wide geographic area (Chapman et al., in review), it is unlikely that the isotopes reflect mixing of seawater with clastic sediments that make up the shale; it is more likely that some basin-wide process occurred. Evans and Battles (1999) applied fluid inclusion and stable isotope analyses to identify two separate fluid migration events in the Lower to Middle Devonian strata of this region.

Unlike the Marcellus Shale samples, the ε_{Sr} value of the acetic acid leach of sample 6, proposed to be the Tully Limestone, does reach the range for Middle Devonian seawater. This indicates that some original carbonate material may be present in this sample.

The HCl leachates extracted Sr with higher ε_{Sr} values, indicating dissolution of more radiogenic Sr-bearing minerals. This Sr could originate from the partial dissolution of clastic silicate material such as clays and other detrital minerals.

4.4.3 Rb-Sr isotope mixing correlations

In Figure 26, ε_{Sr} is plotted against the Rb/Sr ratio, which can be used to identify mixing between radiogenic and non-radiogenic Sr components. The Rb-Sr isotope system correlation of carbonate minerals demonstrates a mixture between less radiogenic and more radiogenic components, and indicates that there has been more than one generation of carbonate precipitation. The intercept for this curve is the ε_{Sr} for seawater at the time of deposition and represents the original carbonate material. This original marine carbonate, which contained seawater-derived Sr with an ε_{Sr} value near -12, mixed with a more radiogenic ($\varepsilon_{Sr} > +10$) endmember from a non-marine source. The more radiogenic endmember, likely a basin-wide migrating fluid (see discussion above), caused dissolution of the original carbonate and re-precipitation of carbonate minerals containing Sr with higher ε_{Sr} values. Fluid inclusions in calcite and barite veins of the Marcellus Shale also exhibit evidence of up to five separate mineralizing events (Evans et al., submitted).

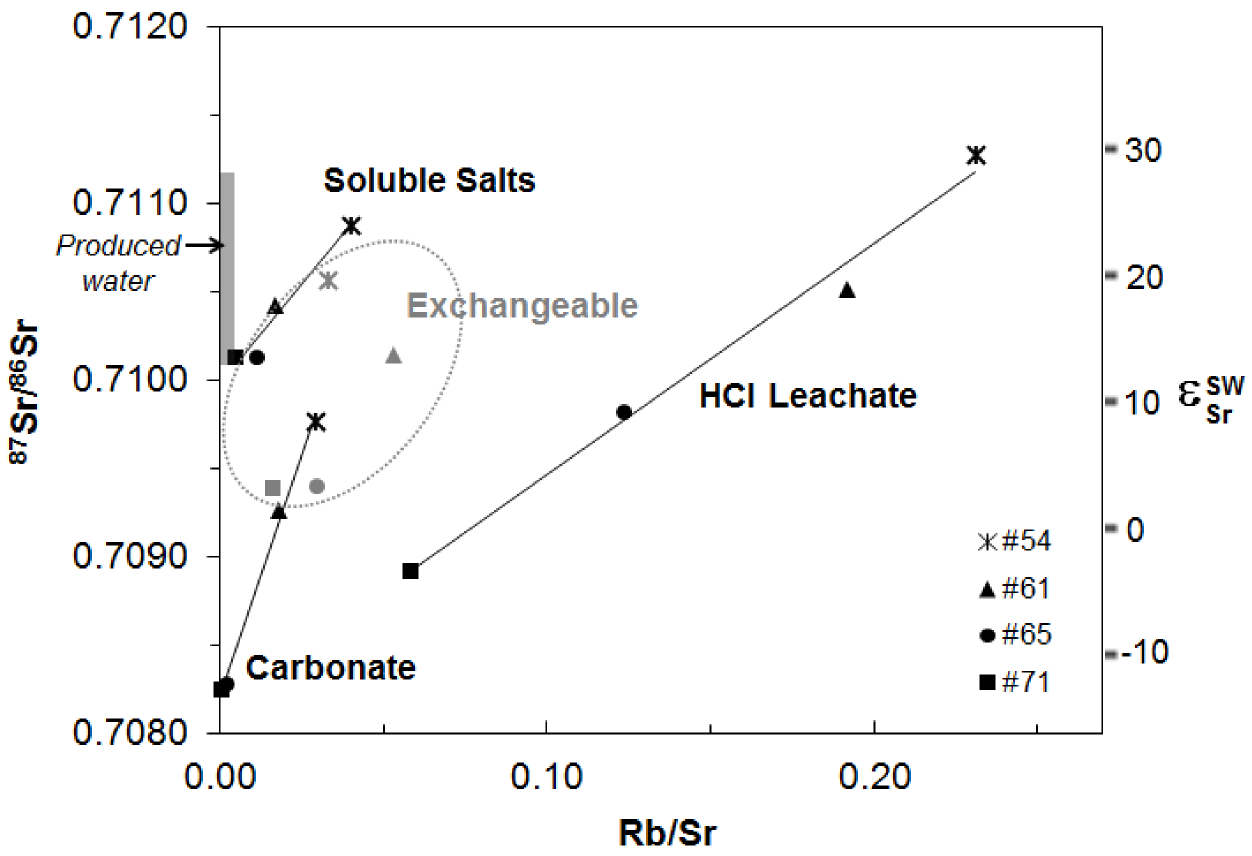

Figure 26. Sr isotopic values vs. Rb/Sr for Marcellus Shale samples. Curve labeled 'Soluble Salts' comprises water leachates; curve labeled 'Carbonate' comprises acetic acid leachates; curve labeled 'Exchangeable' comprises ammonium leachates. The straight-line correlations depict mixing between radiogenic and non-radiogenic components. The intercept for the Carbonate curve falls within the range of ε_{Sr} for Middle Devonian seawater.

The correlation for soluble salts shows that the water leach did not access any remnants of the original seawater salt component. Rather, the original ε_{Sr} signature has been more thoroughly overprinted by a subsequent radiogenic component. This is to be expected, because salts are generally more water-soluble than carbonates. Nevertheless, a linear correlation is observed, which demonstrates that a mixing process has taken place. Limited Rb/Sr data for Marcellus produced waters suggest that these waters have very low Rb/Sr (shown by the shaded region on Figure 26); and, as discussed earlier, the leaches which targeted soluble salts had ε_{Sr} values within the range of these produced waters.

The exchangeable ions liberated in the ammonium acetate leach have more variable Rb-Sr isotope systematics, indicating that sorption processes, rather than mineral dissolution and precipitation, were occurring. Sorption and cation exchange readily operate on the surface of clay minerals, which appear to be present in all portions of the Marcellus Shale (see Table 7).

The HCl leach, which targeted phases which would be soluble in dilute acid, also shows clear evidence of mixing. This leach may have caused partial dissolution of some silicate minerals, but the intercept for this curve falls near the intercept for carbonate minerals, indicating that some residual carbonate material may have dissolved along with the more radiogenic silicate component.

4.5 CONCLUSIONS AND SUGGESTIONS FOR FUTURE WORK

A comparison of ε_{Sr} values for water and ammonium acetate leachates of the Marcellus Shale to the ε_{Sr} signature of produced waters suggests that the dissolved solids in Marcellus Shale produced waters most likely originate from within the shale itself, and are not derived from adjacent, high porosity units. This has implications in understanding the composition of the shale, including any autochthonous salts and/or formation brines. An understanding of salt heterogeneities in the unit can guide drilling and remediation strategies.

The upper and lower portions of the Marcellus Shale have different mineralogical compositions, primarily in terms of carbonate content. This mineralogy affects the release of Ca and Sr from the shale, with most of the Ca and Sr in the lower, more carbonate-rich shale being released with acetic acid. This suggests that any addition of dilute acid to the hydrofracturing fluid (GWPC and ALL Cons., 2009) may release additional amounts of these elements from carbonate reservoirs. The extraction of the majority of Ba with the ammonium acetate leach suggests that Ba is stored in clay exchangeable sites or as barite; the high ionic strength of the hydraulic fracturing fluid may enhance its ability to release significant amounts of Ba from the shale.

Finally, evidence is presented of more than one generation of carbonate precipitation in the shale, as well as mixing of the original seawater-derived components with a later, more radiogenic source. Because of the relatively narrow range of produced water ε_{Sr} values over an extensive geographic area, the more radiogenic source must have been spread over a large region, possibly in the form of a basin-wide brine or other fluid.

To gain more information on the nature of metals and salts in the Marcellus Shale, additional cores from other areas of the shale should be studied. In particular, cores from areas with different thermal maturity or in different portions of the Acadian clastic wedge could provide insight into heterogeneities within the shale. Additionally, dissolution of limestone endmembers, such as verified samples of the Onondaga or Tully Limestone, would provide Sr isotopic data for Middle Devonian marine limestone.

5.0 CONCLUDING REMARKS

5.1 MAJOR CONCLUSIONS

The three studies presented in this dissertation are intended as pilot studies to establish the importance of integrating geology, geochemistry, and isotopes in understanding water-rock interaction. These pilot studies were designed to establish techniques and analyses that can be used in future applications. While this research was performed on locations within the Appalachian Basin, its results have widespread applicability to other geologically complex regions in which fossil fuel extraction takes place, such as the Powder River Basin in Wyoming, coal mining regions in China and England, and shale gas reservoirs in the central US. Additionally, the isotope tracking techniques described are relevant to monitoring and detection strategies in CO_2 sequestration.

In the first project, geochemistry and Sr isotopes were used to distinguish between shallow and deep contaminant sources, as well as between sources related to different fossil fuels (coal vs. oil and natural gas). Iron-rich waters flowing from abandoned oil and natural gas wells were shown to result from shallow migration of AMD into gas wells via compromised well casings, a potentially major issue in historic oil- and gas-producing regions. The application of Sr isotopes, combined with an understanding of subsurface stratigraphy and geology, demonstrated that dissolution of siderite cement in a shallow aquifer contributed to the high iron content of these waters. In addition to clarifying this mixing pathway and dissolution process, Sr isotopes allowed for quantification of the mixing of groundwater, AMD, and siderite.

The second study characterized the Sr isotopic composition of Marcellus Shale produced waters, and showed that these waters fall in a narrow range of ε_{Sr} values that are above the range for marine limestone. This narrow isotopic range over large geographic distances suggests that basin-wide processes led to the homogenization of Sr isotopes. The difference between ε_{Sr} values of Marcellus Shale produced waters and marine limestone suggests that post-depositional processes altered the original marine material.

Additionally, it was shown that Sr isotopes can distinguish between Marcellus Shale produced waters and western Pennsylvania AMD, as well as Upper Devonian Venango brines; these sources can be further distinguished by combining Sr isotopes with a distinguishing chemical parameter (such as Sr/Ca). As in the first study, Sr isotopes were shown to be able to distinguish between possible contaminant sources as well as quantify the contribution of each source. Time-series data from Marcellus Shale gas wells suggests that Sr isotopes might also be useful in detecting hydrofracturing excursions into adjacent stratigraphic units.

In the third study, sequential extraction of Marcellus Shale drill cuttings identified reservoirs of major cations seen in produced waters. For the major elements observed in Marcellus produced waters, the following reservoirs are inferred from this study: Na - soluble salts; Ca - carbonates; Sr - either exchangeable sites or carbonates; Ba - either exchangeable sites or a phase, such as barite, only released with high-ionic strength fluids. The extractions, combined with XRD data, demonstrated compositional differences between the upper and lower members of the Marcellus Shale. Strontium isotopic analysis of the leachates showed that the dissolved solids in Marcellus Shale produced waters most likely originate within the shale itself, rather than in adjacent units. Additionally, these isotopic values suggested that more than one generation of mineral precipitation and dissolution has occurred in the Marcellus Shale. Plots of ε_{Sr} vs. Rb/Sr illustrate mixing of the original carbonate and salt components with a later, more radiogenic component.

5.2 RECOMMENDATIONS FOR FUTURE WORK

The research presented in this dissertation suggests the following directions for further application of geology, geochemistry, and isotopes:

- Based on its demonstrated utility in clarifying subsurface processes, the Sr isotopic system could be applied to the monitoring of interactions between fluids and rocks in carbon sequestration projects.
- To allow for more sensitive and robust tracking of Marcellus Shale produced waters, Sr isotopes can be integrated with other isotope systems (e.g., C, O, H, B, S, Li, and Nd).
- A list compiling the Sr isotopic composition of more possible Appalachian Basin high-TDS endmembers, including road salt, fertilizer, eastern U.S. coalbed methane produced waters, and fly ash-related waters (e.g., Spivak-Birndorf et al., in press), could be helpful in tracking contamination sources.
- Background geochemical and isotopic data could be collected for ground and surface water in areas that are likely to be sites of future Marcellus Shale gas drilling.
- Mechanisms for fluid flow in the Marcellus Shale could be further investigated through the analysis of other cores, as well as structural features and fluid inclusions (e.g., Evans, 2011).

- Additional cores from a wide geographic region could also be helpful in characterizing geochemical and isotopic homogeneity across the Appalachian Basin.
- Research combining geochemistry and isotopes can be extended to possible future shale gas plays, particularly the Utica Shale.

BIBLIOGRAPHY

Armstrong, S.C., Sturchio, N.C., and Hendry, M.J., 1998, Strontium isotopic evidence on the chemical evolution of pore waters in the Milk River Aquifer, Alberta, Canada: Applied Geochemistry, v. 13, p. 463-475.

Arthur, J.D., Bohm, B., and Layne, M., 2008, Hydraulic fracturing considerations for natural gas wells of the Marcellus Shale, The Ground Water Protection Council 2008 Annual Forum: Cincinnati, OH, ALL Consulting.

Baldassare, F.J., and Laughrey, C.D., 1997, Identifying the sources of stray methane by using geochemical and isotopic fingerprinting: Environmental Geosciences, v. 4, p. 85-94.

Banner, J.L., Musgrove, M., and Capo, R.C., 1994, Tracing ground-water evolution in a limestone aquifer using Sr isotopes: Effects of multiple sources of dissolved ions and mineral-solution reactions: Geology, v. 22, p. 687-690.

Banner, J.L., Wasserburg, G.J., Dobson, P.F., Carpenter, A.B., and Moore, C.H., 1989, Isotopic and trace element constraints on the origin and evolution of saline groundwaters from central Missouri: Geochimica et Cosmochimica Acta, v. 53, p. 383-398.

Barnaby, R.J., Oetting, G.C., and Gao, G., 2004, Strontium isotopic signatures of oil-field waters: Applications for reservoir characterization: AAPG Bulletin, v. 88, p. 1677-1704.

Basan, P.B., Kissling, D.L., Hemsley, K.D., Kersey, D.G., Dow, W.G., Chaiffetz, M.S., Isaacson, P., Barrett, S., and Carne, L., 1980, Geological study and reservoir evaluation of Early Devonian formations of the Appalachians: Houston, TX, Robertson Research Inc., p. 263.

Bayless, R.E., Bullen, T.D., and Fitzpatrick, J.A., 2004, Use of 87Sr/86Sr and d11B to identify slag-affected sediment in southern Lake Michigan: Environmental Science & Technology, v. 38, p. 1330-1337.

Berner, E.K., and Berner, R.A., 1996, Global environment: Water, air and geochemical cycles: Upper Saddle River, NJ, Prentice Hall, 376 p.

Blauch, M.E., Myers, R.R., Moore, T.R., Lipinski, B.A., and Houston, N.A., 2009, Marcellus shale post-frac flowback waters - Where is all the salt coming from and what are the implications?, Society of Petroleum Engineers Eastern Regional Mtg.: Charleston, WV, p. 221-240.

Blount, C.W., 1977, Barite solubilities and thermodynamic quantities up to 300 degrees C and 1400 bars: American Mineralogist, v. 62, p. 942-957.

Brady, K.B.C., 1998, Groundwater chemistry from previously mined areas as a mine drainage prediction tool, in Brady, K.B.C., Smith, M.J., and Schueck, J., eds., Coal Mine Drainage Prediction and Pollution Prevention in Pennsylvania: Harrisburg, PA, PA DEP, p. 9-1 to 9-21.

Brady, K.B.C., Hornberger, R.J., and Fleeger, G., 1998, Influence of geology on postmining water quality: northern Appalachian Basin, *in* Brady, K.B.C., Smith, M.J., and Schueck, J., eds., Coal Mine Drainage Prediction and Pollution Prevention in Pennsylvania: Harrisburg, PA, PA DEP, p. 8-1 to 8-92.

Brenot, A., Baran, N., Petelet-Giraud, E., and Négrel, P., 2008, Interaction between different water bodies in a small catchment in the Paris basin (Brévilles, France): Tracing of multiple Sr sources through Sr isotopes coupled with Mg/Sr and Ca/Sr ratios: Applied Geochemistry, v. 23, p. 58-75.

Brett, C.E., and Baird, G.C., 1996, Middle Devonian sedimentary cycles and sequences in the northern Appalachian Basin: Geological Society of America Special Papers, v. 306, p. 213-241.

Brinck, E.L., and Frost, C.D., 2007, Detecting infiltration and impacts of introduced water using strontium isotopes: Ground Water, v. 45, p. 554-568.

Burke, W.H., Denison, R.E., Hetherington, E.A., Koepnick, R.B., Nelson, H.F., and Otto, J.B., 1982, Variation of seawater $^{87}Sr/^{86}Sr$ throughout Phanerozoic time: Geology, v. 10, p. 516-519.

California Department of Conservation (CA DOC), 1986, A study of abandoned oil and gas wells and methane and other hazardous gas accumulations, Report SB 1458: Sacramento, CA.

Capo, R.C., Stewart, B.W., and Chadwick, O.A., 1998, Strontium isotopes as tracers of ecosystem processes: theory and methods: Geoderma, v. 82, p. 197-225.

Capo, R.C., Winters, R.W., Weaver, T.J., Stafford, S.L., Hedin, R.S., and Stewart, B.W., 2001, Hydrogeologic and geochemical evolution of deep mine discharges, Irwin Syncline, Pennsylvania: Proc 22nd West Virginia Surface Mine Drainage Task Force Symp, p. 144-153.

Carlson, E.H., 1987, Celestite replacements of evaporites in the Salina Group: Sedimentary Geology, v. 54, p. 93-112.

Calvo, R., Ayalon, A., Bein, A., and Sass, E., 2011, Chemical and isotopic composition of diagenetic carbonate cements and its relation to hydrocarbon accumulation in the Heletz-Kokhav oil field (Israel): Journal of Geochemical Exploration, v. 108, p. 88-98.

Chapman, E.C., Capo, R.C., Stewart, B.W., Hedin, R.S., Weaver, T.J., and Edenborn, H.M., in prep, Strontium isotope quantification of siderite, brine, and acid mine drainage contributions to abandoned gas well discharges in the Appalachian Plateau: Applied Geochemistry.

Chapman, E.C., Capo, R.C., Stewart, B.W., Kirby, C.S., Hammack, R.W., Schroeder, K.T., and Edenborn, H.M., in review, Geochemical and strontium isotope characterization of produced waters from Marcellus Shale natural gas extraction: Environmental Science & Technology.

Chesnut, D.R., 1996, Geologic framework for the coal-bearing rocks of the Central Appalachian Basin: International Journal of Coal Geology, v. 31, p. 55-66.

Chilingar, G.V., and Endres, B., 2005, Environmental hazards posed by the Los Angeles Basin urban oilfields: An historical perspective of lessons learned: Environmental Geology, v. 47, p. 302-317.

Christian, L.N., Banner, J.L., and Mack, L.E., 2011, Sr isotopes as tracers of anthropogenic influences on stream water in the Austin, Texas, area: Chemical Geology, v. 282, p. 84-97.

Cravotta III, C.A., 2008, Dissolved metals and associated constituents in abandoned coal-mine discharges, Pennsylvania, USA. Part 1: Constituent quantities and correlations: Applied Geochemistry, v. 23, p. 166-202.

Cravotta III, C.A., Brady, K.B.C., Rose, A.W., and Douds, J.B., 1999, Frequency distribution of the pH of coal-mine drainage in Pennsylvania, *in* Morganwalp, D.W., and Buxton, H., eds., US Geological Survey Toxic Substances Hydrology Program – Proceedings of the Technical Meeting, US Geological Survey Water-Resources Investigative Report 99-4018A, p. 313–324.

Dresel, P.E., and Rose, A.W., 2010, Chemistry and origin of oil and gas well brines in western Pennsylvania, Pennsylvania Geological Survey Open-File Oil and Gas Report 10-01.0: Harrisburg, PA.

Ellingboe, J., and Wilson, J., 1964, A quantitative separation of non-carbonate minerals from carbonate minerals: Journal of Sedimentary Petrology, v. 34, p. 412-418.

Engelder, T., Lash, G.G., and Uzcátegui, R.S., 2009, Joint sets that enhance production from Middle and Upper Devonian gas shales of the Appalachian Basin: AAPG Bulletin, v. 93, p. 857-889.

Evans, M.A., 2011, Deformation and fluid history of the Marcellus Shale in the Pennsylvania Valley and Ridge: Evidence from fluid inclusion microthermometry of vein minerals, Geological Society of America Northeastern/North-Central Joint Meeting: Pittsburgh, PA.

Evans, M.A., and Battles, D.A., 1999, Fluid inclusion and stable isotope analyses of veins from the central Appalachian Valley and Ridge province: Implications for regional synorogenic hydrologic structure and fluid migration: Geological Society of America Bulletin, v. 111, p. 1841-1860.

Evans, M.A., Leo, J., and Burruss, R.C., submitted, 2012, Spatial and temporal variation of fluids in the Devonian Marcellus Shale during deformation of the central Appalachian fold-and-thrust belt, Geofluids International Conference: Rueil-Malmaison, France.

Frost, C.D., Brinck, E.L., Mailloux, J., Sharma, S., Campbell, C.E., Carter, S.A., and Pearson, B.N., 2010, Innovative approaches for tracing water co-produced with coalbed natural gas: Applications of strontium and carbon isotopes of produced water in the Powder River Basin, Wyoming and Montana, *in* Reddy, K.J., ed., Coalbed Natural Gas: Energy and Environment: Hauppauge, NY, Nova Science Publishers, Inc.

Frost, C.D., Pearson, B.N., Ogle, K.M., Heffern, E.L., and Lyman, R.M., 2002, Sr isotope tracing of aquifer interactions in an area of accelerating coal-bed methane production, Powder River Basin, Wyoming: Geology, v. 30, p. 923-926.

Frost, C.D., and Toner, R.N., 2004, Strontium isotopic identification of water-rock interaction and ground water mixing: Ground Water, v. 42, p. 418-432.

Giddens, P.H., 1947, Pennsylvania Petroleum, 1760-1872: Titusville, PA, Drake Well Memorial Park, 420 p.

Ground Water Protection Council (GWPC) and ALL Consulting, 2009, Modern shale gas development in the United States: A primer, Prepared for the US Department of Energy: Oklahoma City, OK.

Graustein, W.C., 1989, ^{87}Sr/^{86}Sr ratios measure the sources and flow of strontium in terrestrial ecosystems, *in* Rundel, P.W., Ehleringer, J.R., and Nagy, K.A., eds., Stable Isotopes in Ecological Research: New York, Springer-Verlag, p. 491-512.

Hamel, B.L., Stewart, B.W., and Kim, A.G., 2010, Tracing the interaction of acid mine drainage with coal utilization byproducts in a grouted mine: Strontium isotope study of the inactive Omega Coal Mine, West Virginia (USA): Applied Geochemistry, v. 25, p. 212-223.

Hammack, R., Kaminski, V., Harbert, W., Veloski, G., and Lipinski, B., 2010, Using helicopter electromagnetic (HEM) surveys to identify potential hazards at coal-waste impoundments: Examples from West Virginia: Geophysics, v. 75, p. B221-229.

Harbert, W., and Kaminski, V., 2007, Methane emissions project, Borough of Versailles, Pennsylvania: Seismic reflection study, Prepared for Department of Energy National Energy Technology Laboratory: Pittsburgh, PA.

Harper, J., 2008, The Marcellus Shale: an old "new" gas reservoir in Pennsylvania, Pennsylvania Geology, Volume 28, Bureau of Topographic and Geologic Survey, Pennsylvania Department of Conservation and Natural Resources: Pittsburgh, PA.

Harper, J., and Kostelnik, J., 2010, The Marcellus Shale play in Pennsylvania, Online report to Pennsylvania Department of Conservation and Natural Resources, http://www.dcnr.state.pa.us/topogeo/oilandgas/Marcellus.pdf.

Harper, J., and Ward, A.N., Jr., 1999. Rocks, oil, gravel, iron: the surficial, bedrock, and economic geology of Venango County: Pittsburgh Geological Society, Pittsburgh, PA.

Hawkins, J.W., 1998, Hydrogeologic characteristics of surface-mine spoil, *in* Brady, K.B.C., Smith, M.J., and Schueck, J., eds., Coal Mine Drainage and Pollution Prevention in Pennsylvania: Harrisburg, PA, PA DEP, p. 3-1 to 3-11.

Hedin, R.S., Stafford, S.L., and Weaver, T.J., 2005, Acid mine drainage flowing from abandoned gas wells: Mine Water and the Environment, v. 24, p. 104-106.

Jiang, Y., Wu, Y., and Yuan, D., 2009, Human impacts on karst groundwater contamination deduced by coupled nitrogen with strontium isotopes in the Nandong underground river system in Yunan, China: Environmental Science & Technology, v. 43, p. 7676-7683.

Johnson, J.D., and Graney, J.R., 2011, Coupling lead isotope ratios and element concentrations to track processes involved in resource extraction from the Marcellus Shale, Geological Society of America Annual Meeting: Minneapolis, MN.

Kaplan, I.R., Galperin, Y., Lu, S.-T., and Lee, R.-P., 1997, Forensic environmental geochemistry: Differentiation of fuel-types, their sources and release time: Organic Geochemistry, v. 27, p. 289-317.

Kargbo, D.M., Wilhelm, R.G., and Campbell, D.J., 2010, Natural gas plays in the Marcellus Shale: Challenges and potential opportunities: Environmental Science & Technology, v. 44, p. 5679-5684.

Karim, A., Pe-Piper, G., and Piper, D.J.W., 2010, Controls on diagenesis of Lower Cretaceous reservoir sandstones in the western Sable Subbasin, offshore Nova Scotia: Sedimentary Geology, v. 224, p. 65-83.

Keister, T., 2010, Marcellus hydrofracture flowback and production wastewater treatment, recycle, and disposal technologies, The Science of Marcellus Shale: Williamsport, PA.

Kerr, R.A., 2010, Natural gas from shale bursts onto the scene: Science, v. 328, p. 1624-1626.

Kharaka, Y.K., Thordsen, J.J., Kakouros, E., and Abbott, M.M., 2003. Environmental impacts of petroleum production: Fate of inorganic and organic chemicals in produced water from the Osage-Skiatook Petroleum Environmental Research sites, Osage County, Oklahoma: Water-Resources Investigations Report 03-4260. U.S. Geological Survey, p. 56-83.

Kight, M.D., and Siegel, D.I., 2011, A protocol to characterize flowback water contamination to shallow waters from shale gas development, Northeastern and North-Central Joint Meeting of the Geological Society of America, Volume 43: Pittsburgh, PA, Geological Society of America, p. 76.

Lash, G.G., 2008, The influence of basin dynamics on depositional patterns of the Middle Devonian Marcellus Shale, western New York and northwestern Pennsylvania: American Association of Petroleum Geologists Annual Convention: San Antonio, TX, p. 116.

Lash, G.G., and Engelder, T., 2009, The middle Devonian Marcellus shale - a record of eustasy and basin dynamics: National Meeting of the American Association of Petroleum Geologists: Denver, CO.

Lash, G.G., and Engelder, T., 2011, Thickness trends and sequence stratigraphy of the Middle Devonian Marcellus Formation, Appalachian Basin: Implications for Acadian foreland basin evolution: AAPG Bulletin, v. 95, p. 61-103.

Laughrey, C.D., and Baldassare, F.J., 1998, Geochemistry and origin of some natural gases in the Plateau Province, central Appalachian Basin, Pennsylvania and Ohio: AAPG Bulletin, v. 82, p. 317-335.

Leggette, R.M., 1936. Ground Water in Northwestern Pennsylvania: Topographic and Geologic Survey, Harrisburg, PA.

Leung, C.M., and Jiao, J.J., 2006, Use of strontium isotopes to identify buried water main leakage into groundwater in a highly urbanized coastal area: Environmental Science & Technology, v. 40, p. 6575-6579.

Love, E., Hammack, R., Harbert, W., Sams, J., Veloski, G., and Ackman, T., 2005, Using airborne thermal infrared imagery and helicopter EM conductivity to locate mine pools and discharges in the Kettle Creek watershed, north-central Pennsylvania: Geophysics, v. 70, p. B73-81.

McMahon, P.B., Cowdery, T.K., Chapelle, F.H., and Jurgens, B.C., 2009. Redox conditions in selected principal aquifers of the United States: U.S. Geological Survey Fact Sheet 2009-3041.

McNutt, R.H., Frape, S.K., and Dollar, P., 1987, A strontium, oxygen and hydrogen isotopic composition of brines, Michigan and Appalachian basins, Ontario and Michigan: Applied Geochemistry, v. 2, p. 495-505.

Merritt, G.L., and Emrich, G.H., 1970, The need for hydrogeologic evaluations in a mine drainage abatement program: A case study, Toms Run, Clarion County, Pennsylvania, *in* C.T., H., ed., 3rd Symposium on Coal Mine Drainage Research: Mellon Institute, Pittsburgh, PA, p. 334-364.

Milici, R.C., and Swezey, C.S., 2006, Assessment of Appalachian Basin oil and gas resources: Devonian shale - Middle and Upper Paleozoic total petroleum system: U.S. Geological Survey Open-File Report 2006-1237, Reston, VA.

Millot, R., Guerrot, C., Innocent, C., Négrel, P., and Sanjuan, B., 2011, Chemical, multi-isotopic (Li–B–Sr–U–H–O) and thermal characterization of Triassic formation waters from the Paris Basin: Chemical Geology, v. 283, p. 226-241.

Monea, M., Knudsen, R., Worth, K., Chalaturnyk, R., White, D., Wilson, M., Plasynski, S., McIlvried, H.G., and Srivastava, R.D., 2009. Considerations for monitoring, verification, and accounting for geologic storage of CO_2, Carbon Sequestration and Its Role in the Global Carbon Cycle: American Geophysical Union Monograph 183, p. 303-316.

Morad, S., 1998, Carbonate Cementation in Sandstones: Distribution Patterns and Geochemical Evolution, Special Publication 26 of the International Assoc. of Sedimentologists Series, Blackwell Science Ltd.: Oxford, England.

Mullaney, J.R., Lorenz, D.L., and Arntson, A.D., 2009, Chloride in groundwater and surface water in areas underlain by the glacial aquifer system, northern United States: U.S. Geological Survey Scientific Investigations Report 2009-5086, Reston, VA.

National Energy Technology Laboratory (NETL), 2009. Best practices for monitoring, verification, and accounting of CO_2 stored in deep geologic formations: DOE/NETL Report 311/081508, Morgantown, WV.

New York State Department of Environmental Conservation (NYSDEC), 2011, Supplemental generic environmental impact statement on the oil, gas and solution mining regulatory program: Albany, NY.

Osborn, S.G., and McIntosh, J.C., 2010, Chemical and isotopic tracers of the contribution of microbial gas in Devonian organic-rich shales and reservoir sandstones, northern Appalachian Basin: Applied Geochemistry, v. 25, p. 456-471.

Osborn, S.G., Vengosh, A., Warner, N.R., and Jackson, R.B., 2011a, Methane contamination of drinking water accompanying gas-well drilling and hydraulic fracturing: Proceedings of the National Academy of Sciences, v. 108, p. 8172-8176.

Osborn, S.G., Vengosh, A., Warner, N.R., and Jackson, R.B., 2011b, Reply to Saba and Orzechowski and Schon: Methane contamination of drinking water accompanying gas-well drilling and hydraulic fracturing: Proceedings of the National Academy of Sciences, v. 108, p. E665-E666.

Paytan, A., Averyt, K., Faul, K., Gray, E., and Thomas, E., 2007, Barite accumulation, ocean productivity, and Sr/Ba in barite across the Paleocene-Eocene Thermal Maximum: Geology, v. 35, p. 1139-1142.

Penn State Marcellus Center for Outreach and Research (MCOR), 2011, Depth of Marcellus Shale base, http://www.marcellus.psu.edu/images/Marcellus_Depth.gif.

Pennsylvania Department of Environmental Protection (PA DEP), 1992, Pennsylvania Mining History: Harrisburg, PA.

Pennsylvania Department of Environmental Protection (PA DEP), 2000, Pennsylvania's Plan for Addressing Problem Abandoned Wells and Orphaned Wells: Harrisburg, PA.

Pennsylvania Department of Environmental Protection (PA DEP), 2007, Orphan oil and gas wells and the orphan well plugging fund: Harrisburg, PA.

Pennsylvania Department of Environmental Protection (PA DEP), 2009, Pennsylvania Nonpoint Source Management Program FFY2008 Annual Report: Harrisburg, PA.

Pennsylvania Department of Environmental Protection (PA DEP), 2010, 2009 Year End Workload Report: Harrisburg, PA.

Pennsylvania Fish and Boat Commission (PFBC), 2011, Press Release: PA Fish and Boat Commission sues Consol Energy over Dunkard Creek environmental disaster.

Perry, E.F., 2001, Modeling rock-water interactions in flooded underground coal mines, Northern Appalachian Basin: Geochemistry: Exploration, Environment, Analysis, v. 1, p. 61-70.

Perry Jr, E.A., and Turekian, K.K., 1974, The effects of diagenesis on the redistribution of strontium isotopes in shales: Geochimica et Cosmochimica Acta, v. 38, p. 929-935.

Peterman, Z.E., Thamke, J.N., Futa, K., and Oliver, T.A., 2010, Strontium isotope detection of brine contamination in the East Poplar oil field, Montana: U.S. Geological Society Open-File Report 2010-1326, p. 20.

Poth, C.W., 1962, The occurrence of brine in western Pennsylvania, Bulletin M-47: Harrisburg, PA, Pennsylvania Geological Survey, p. 53.

Querol, X., Klika, Z., Weiss, Z., Finkelman, R.B., Alastuey, A., Juan, R., Lopez-Soler, A., Plana, F., Kolker, A., and Chenery, S.R.N., 2001, Determination of element affinities by density fractionation of bulk coal samples: Fuel, v. 80, p. 83-96.

Renner, R., 2009a, Pennsylvania to regulate salt discharges: Environmental Science & Technology, v. 43, p. 6120.

Renner, R., 2009b, Salt-loving algae wipe out fish in Appalachian stream: Environmental Science & Technology, v. 43, p. 9046-9047.

Révész, K.M., Breen, K.J., Baldassare, A.J., and Burruss, R.C., 2010, Carbon and hydrogen isotopic evidence for the origin of combustible gases in water-supply wells in north-central Pennsylvania: Applied Geochemistry, v. 25, p. 1845-1859.

Reynolds, L., 2009, Update on Dunkard Creek: November 23, 2009, U.S. EPA Freshwater Biology Team Report, p. 17.

Risthaus, P., Bosbach, D., Becker, U., and Putnis, A., 2001, Barite scale formation and dissolution at high ionic strength studied with atomic force microscopy: Colloids and Surfaces A: Physicochemical and Engineering Aspects, v. 191, p. 201-214.

Rose, A.W., and Cravotta, C.A., 1998, Geochemistry of coal mine drainage, *in* Brady, K.B.C., Smith, M.J., and Schueck, J., eds., Coal Mine Drainage Prediction and Pollution Prevention in Pennsylvania: Harrisburg, PA, PA DEP, p. 1-1 to 1-22.

Rowan, E.L., 2011, Inorganic chemistry of produced water in the Appalachian Basin, EPA Technical Workshop for the Hydraulic Fracturing Study: Chemical & Analytical Methods: Arlington, VA, p. 10-13.

Rowan, E.L., and De Marsily, G., 2001, Infiltration of late Palaeozoic evaporative brines in the Reelfoot rift: A possible salt source for Illinois Basin formation waters and MVT mineralizing fluids: Petroleum Geoscience, v. 7, p. 269-279.

Rowe, D., and Muehlenbachs, K., 1999, Isotopic fingerprints of shallow gases in the Western Canadian sedimentary basin: Tools for remediation of leaking heavy oil wells: Organic Geochemistry, v. 30, p. 861-871.

Ryder, R.T., 1995, Appalachian Basin Province (067), *in* Gautier, D.L., Dolton, G.L., Takahashi, K.I., and Varnes, K.L., eds., 1995 National Assessment of United States Oil and Gas Resources: Results, Methodology, and Supporting data, U.S. Geological Survey Digital Data Series DDS-30, p. 144.

Saba, T., and Orzechowski, M., 2011. Lack of data to support a relationship between methane contamination of drinking water wells and hydraulic fracturing: Proceedings of the National Academy of Sciences, online only.

Schoell, M., 1980, The hydrogen and carbon isotopic composition of methane from natural gases of various origins: Geochimica et Cosmochimica Acta, v. 44, p. 649-661.

Schoell, M., 1983, Genetic characterization of natural gases: AAPG Bulletin, v. 67, p. 2225-2238.

Schon, S.C., 2011. Hydraulic fracturing not responsible for methane migration. Proceedings of the National Academy of Sciences, online only.

Sharma, S., and Frost, C.D., 2008, Tracing coalbed natural gas–coproduced water using stable isotopes of carbon: Ground Water, v. 46, p. 329-334.

Sharma, S., Mulder, M.L., Edenborn, H.M., and Hammack, R.W., 2011, Stable isotope fingerprinting of co-produced waters associated with Marcellus shale natural gas extraction, Annual Meeting of the Geological Society of America: Minneapolis, MN.

Shultz, C.H., 1999, The Geology of Pennsylvania: Harrisburg, PA and Pittsburgh, PA, Pennsylvania Geological Survey and Pittsburgh Geological Society, 888 p.

Skousen, J., Renton, J., Brown, H., Evans, P., Leavitt, B., Brady, K., Cohen, L., and Ziemkiewicz, P., 1997, Neutralization potential of overburden samples containing siderite: Journal of Environmental Quality, v. 26, p. 673-681.

Spivak-Birndorf, L.J., Stewart, B.W., Capo, R.C., Chapman, E.C., and Brubaker, T.M., in press, Strontium isotope study of coal utilization byproducts interacting with environmental waters: Journal of Environmental Quality.

Stueber, A.M., and Walter, L.M., 1991, Origin and chemical evolution of formation waters from Silurian-Devonian strata in the Illinois basin, USA: Geochimica et Cosmochimica Acta, v. 55, p. 309-325.

Stueber, A.M., Walter, L.M., Huston, T.J., and Pushkar, P., 1993, Formation waters from Mississippian-Pennsylvanian reservoirs, Illinois basin, USA: Chemical and isotopic constraints on evolution and migration: Geochimica et Cosmochimica Acta, v. 57, p. 763-784.

Swezey, C.S., 2002, Regional stratigraphy and petroleum systems of the Appalachian Basin, North America, U.S. Geological Survey Geologic Investigations Series Map I-2768.

Uliana, M.M., Banner, J.L., and Sharp Jr, J.M., 2007, Regional groundwater flow paths in Trans-Pecos, Texas inferred from oxygen, hydrogen, and strontium isotopes: Journal of Hydrology, v. 334, p. 334-346.

United States Energy Information Administration (U.S. EIA), 2011a, Marcellus Shale gas play, Appalachian Basin, Based on data from WVGES, PA DCNR, OH DGS, NYSDEC, VA DMME, USGS, and Wrightsone, 2009, http://www.eia.gov/oil_gas/rpd/shaleusa5.pdf.

United States Energy Information Administration (U.S. EIA), 2011b, Review of emerging resources: U.S. shale gas and shale oil plays: Washington, DC, 82 p.

United States Environmental Protection Agency (U.S. EPA), 2004, Evaluation of impacts to underground sources of drinking water by hydraulic fracturing of coalbed methane reservoirs, Office of Ground Water and Drinking Water report 816-R-04-003: Washington, DC.

United States Environmental Protection Agency (U.S. EPA), 2011, Draft plan to study the potential impacts of hydraulic fracturing on drinking water resources, Office of Research and Development: Washington, DC.

Veatch Jr., R.W., Moschovidis, Z.A., and Fast, C.R., 1989, An overview of hydraulic fracturing, *in* Gidley, J.L., Holditch, S.A., Nierode, D.E., and Veatch Jr., R.W., eds., Recent Advances in Hydraulic Fracturing, Henry L. Doherty Series Monograph Volume 12, Society of Petroleum Engineers.

Wilson, J.M., and VanBriesen, J.M., 2011, Use of Br:Cl ratios to track sources of total dissolved solids in the Monongahela River basin, Northeastern and North-Central Joint Meeting of the Geological Society of America, Volume 43: Pittsburgh, PA, Geological Society of America, p. 154.

Winters, W.R., and Capo, R.C., 2004, Ground water flow parameterization of an Appalachian coal mine complex: Ground Water, v. 42, p. 700-710.

Wyrick, G.G., and Borchers, J.W., 1981. Hydrologic effects of stress-relief fracturing in an Appalachian valley: U.S. Dept. of the Interior, Reston, VA.

Yoxtheimer, D.A., 2011, Water resource management for Marcellus natural gas development, NE-NC Geological Society of America Joint Meeting, Paper No. 16-1: Pittsburgh, PA.

Zoback, M., Kitasei, S., and Copithorne, B., 2010, Addressing the environmental risks from shale gas development: Briefing Paper 1, Worldwatch Institute.